Dissections and trees, with applications to optimal mesh encoding and to random sampling

Éric Fusy and Gilles Schaeffer
Laboratoire d'Informatique de l'École Polytechnique,
LIX, École Polytechnique, 91128 Palaiseau, France
Email: [Eric.Fusy,Gilles.Schaeffer]@lix.polytechnique.fr

Dominique Poulalhon
Laboratoire d'Informatique Algorithmique: Fondements et Applications,
LIAFA, Université Paris 7, 2 place Jussieu, 75251 Paris cedex 05, France
Email: Dominique.Poulalhon@liafa.jussieu.fr

Abstract

We present a bijection between some quadrangular dissections of an hexagon and unrooted binary trees. This correspondence has interesting consequences for enumeration, mesh compression and random graph sampling.

It yields a succinct representation for the set $\mathcal{P}(n)$ of n-edge 3-connected planar graphs matching the entropy bound $\frac{1}{n}\log|\mathcal{P}(n)| = 2 + o(1)$ bits per edge. This solves a theoretical problem in mesh compression, as these graphs abstract the combinatorial part of meshes with spherical topology.

Once the entropy bound is matched, the guaranteed compression rate can only be improved on subclasses: we achieve the optimal parametric rate $\frac{1}{n}\log|\mathcal{P}(n,i,j)|$ bits per edge for graphs of $\mathcal{P}(n)$ with i vertices and j faces. This effectively reduces the entropy as soon as $|i-j| \gg n^{1/2}$, and achieves the optimal rate for triangulations.

It also yields an efficient uniform random sampler for labeled 3-connected planar graphs. Using it, the amortized complexity of sampling labeled planar graphs is reduced from the best previously known $O(n^{6.5})$ to $O(n^3)$.

Preliminary version, do not distribute.
Keywords: planar graphs, trees, bijection, orientations, succinct encodings, mesh compression

1 Introduction

One origin of this work can be traced back to an article of Ed Bender in the American Mathematical Monthly [3], where he asked for a simple explanation of the remarkable asymptotic formula

$$|\mathcal{P}(n,i,j)| \sim \frac{1}{3^5 2^4 ijn}\binom{2i-2}{j+2}\binom{2j-2}{i+2} \qquad (1)$$

for the cardinality of the set of 3-connected planar graphs[1] with i vertices, j faces and $n = i + j - 2$ edges, n going to infinity. By a theorem of Whitney these graphs have essentially a unique embedding on the sphere up to homeomorphisms.

Graphs, dissections and trees Another well known property of 3-connected planar graphs with n edges is the fact that they are in direct one-to-one correspondence with dissections of the sphere into n quadrangles that have no non-facial 4-cycle faces. The heart of our paper lies in a further one-to-one correspondence.

Theorem 1 *There is a one-to-one correspondence between unrooted binary trees with n nodes and quadrangular dissections of an hexagon with n interior vertices and no non-facial 4-cycle.*

The application from binary trees to dissections, which we call *the closure*, is easily described and resembles constructions [27, 6, 25] that were recently proposed for simpler kinds of dissections. Conversely, recovering the tree from the dissection can

[1] Unless when explicitly mentioned, all graphs are unlabeled.

be done in linear time by a traversal akin to Kant's canonical ordering [18, 9, 5, 8]. The proof that these algorithms are correct is rather sophisticated, relying on new properties of constrained orientations as used by Schnyder for triangulations [29] and by Felsner [12] for 3-connected planar graphs.

Theorem 1 leads directly to the implicit representation of the numbers $|P(n,i,j)|$ due to Mullin and Schellenberg and from which Formula 1 derives. It partially explains the combinatorics of the occurrence of the cross product of binomials, since these are typical of bicolored binary tree formulas.

Random sampling A second byproduct of Theorem 1 is an efficient uniform random sampler for labeled 3-connected planar graphs, that is an algorithm that given n – respectively, given (n,i,j) – outputs a random element of $\mathcal{P}(n)$ – respectively, of $\mathcal{P}(n,i,j)$ – with equal chances for all elements.

The uniform random generation of classes of dissections of the sphere like triangulations or 3-connected graphs was first considered in mathematical physics (see refs in [2, 25]), and various types of random planar graphs are commonly used for testing graph drawing algorithms (see [10]).

The best previously known algorithm [28] had expected complexity $O(n^{5/3})$ for $\mathcal{P}(n)$, and was much less efficient for $\mathcal{P}(n,i,j)$, having even exponential complexity for i/j or j/i tending to 2. In Section 9, we show that our generator for $\mathcal{P}(n)$ or $\mathcal{P}(n,i,j)$ performs in linear time except if i/j or j/i tends to 2 where it becomes at most quartic.

From the theoretical point of view, it is also desirable to work with the uniform distribution on planar graphs. However, random planar graphs appear to be challenging mathematical objects [24, 21]. A Markov chain converging to the uniform distribution on planar graphs with i vertices was given in [11], but it resists known approaches for perfect sampling [32], and has unknown mixing time. As opposed to this, a recursive scheme to sample planar graphs was proposed in [4], with amortized complexity $O(n^{6.5})$. This result is based on recursive sampling (aka the method of branching probabilities) [23, 14, 33]. Our new random generator for 3-connected planar graphs allows to reduce the amortized cost to $O(n^3)$.

Succinct representations A second byproduct of Theorem 1 is the possibility to encode in linear time a 3-connected planar graph with n edges by a binary tree with n nodes. In turn the tree can be encoded by a balanced parenthesis word of $2n$ bits. This code is *optimal* in the information theoretic sense: the entropy per edge $\frac{1}{n}\log_2|\mathcal{P}(n)|$ of this class of graphs tends to 2 when n goes to infinity, so that a code for $\mathcal{P}(n)$ cannot give a better guarantee on the compression rate.

Applications calling for compact storage and fast transmission of 3D geometrical meshes have recently motivated a huge literature on compression, in particular for the combinatorial part of the meshes. The first compression algorithms dealt only with triangular faces [26, 30], but many meshes include larger faces, so that polygonal meshes have become prominent (see [1] for a recent survey).

The question of optimality of coders was raised in relation with exception codes produced by several successful heuristics when dealing with meshes with spherical topology [15, 19]. Since these meshes are exactly triangulations (for triangular meshes) and 3-connected planar graphs (for polyhedral ones), the coders of [25] and of the present paper respectively prove that traversal based algorithms can achieve optimality.

On the other hand, in the context of succinct data structures, almost optimal algorithms have been proposed [17, 20], that are based on separator theorems. However these algorithms are not truly optimal (they get ε close to the entropy but at the cost of an uncontrolled increase of the constants in the linear complexity). Moreover, although they rely on a sophisticated recursive structure, they do not support efficient adjacency requests.

As opposed to that, our algorithm shares with [16, 5] the fact that the code produced is essentially the code of a spanning tree. More precisely it is just the balanced parenthesis code of a binary tree, and adjacencies of the initial dissection that are not present in the tree can be recovered from the code by a simple variation on the interpretation of the symbols. Adjacency queries can thus be dealt with in time proportional to the degree of vertices using the approach of [22, 16].

Finally we show that the code can be modified to be optimal on the class $\mathcal{P}(n,i,j)$. Since the entropy of this class is strictly smaller than that

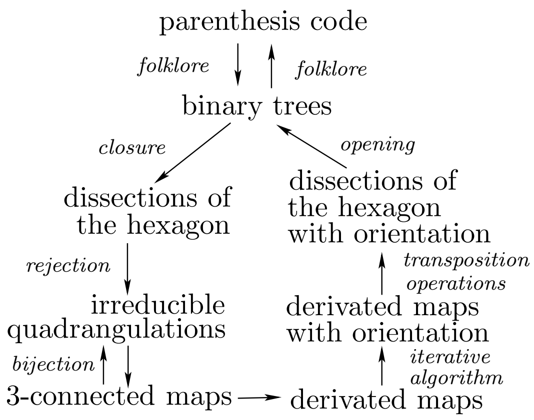

Figure 1: Relations between involved objects.

of $\mathcal{P}(n)$ as soon as $|i - n/2| \gg n^{1/2}$, the resulting parametric coder is more efficient in this range. In particular in the case $j = 2i - 4$ our new algorithm specializes to an optimal coder for triangulations.

Outline of the paper We first present a bijective application between binary trees and some dissections of the hexagon by quadrangular faces; then we deduce from this bijection sampling algorithms for 3-connected planr maps and planar graphs, and finish with the description of a coding algorithm for 3-connected planar maps. The connections between the different families of objects we consider are shown on Figure 1.

2 Definitions

Planar maps A *planar map* is a proper embedding of a connected graph in the plane, where proper means that edges are smooth simple arcs which meet only at their endpoints. A planar map is said *rooted* if one edge of the outer face, called the *root-edge*, is marked and oriented such that the outer face is on the right of the edge. The origin of the root-edge is called *root-vertex*. Vertices are said *outer* or *inner* depending on whether they belong to the outer face or not.

A planar map is said *3-connected* if it can not be disconnected by the removal of two vertices. We denote by $\mathcal{P}'_n$ (resp. $\mathcal{P}'_{ij}$) the set of rooted 3-connected planar maps with n edges (resp.i vertices and j faces).

Plane trees They are planar maps with a single face – the outer one. A vertex is called a *leaf* if it has degree 1, and *node* otherwise. Edges incident to a leaf are called *stems*, and the other *inner edges*. Observe that rooted plane trees are exactly usual trees, with the root-edge oriented from the usual root to its first son. It is convenient anyway to add a *root-leaf* "above" the root-vertex (for symmetry reasons in the case of regular trees). Hence in the following *rooted plane trees* are always rooted on a stem oriented toward its leaf.

Binary trees are plane trees whose nodes have degree 3. We denote respectively by $\mathcal{B}_n$ and $\mathcal{B}'_n$ the sets of binary and rooted binary trees with n nodes (and hence $(n+2)$ leaves).

There is a unique bicoloration of the vertices of a rooted binary tree in black and white such that adjacent vertices have distinct colors and the root-leaf is white. We denote by $\mathcal{B}_{ij}$ and $\mathcal{B}'_{ij}$ the set of (rooted) binary trees with i black nodes and j white nodes for this bicoloration (and hence $2i - j + 1$ white leaves and $2j - i + 1$ black ones).

Quadrangulations and dissections A *quadrangulation* is a planar map whose faces (even the outer face) have degree 4. A *dissection of the hexagon by quadrangular faces* is a planar map whose outer face has degree 6 and inner faces have degree 4.

Any cycle of a map but the one that delimits the outer face is said *proper*. Proper cycles that do not delimit a face are said *separating*.

A quadrangulation or a dissection of the hexagon by quadrangular faces is said *irreducible* if it has no separating 4-cycle. We denote by $\mathcal{Q}_n$ ($\mathcal{Q}'_n$) the set of (rooted) irreducible quadrangulations with n faces (including the outer face, and hence $n+2$ vertices), and by $\mathcal{D}_n$ ($\mathcal{D}'_n$) the set of (rooted) irreducible dissections of the hexagon with n inner vertices (and hence $n+2$ quadrangular faces). From now on, irreducible dissections of the hexagon by quadrangular faces will be shortly called *irreducible dissections*.

As faces of dissections and quadrangulations have even degree, vertices of these maps can be bicolored (say, in black and white), such that each edge connects a black vertex to a white one, and such a bicoloration is unique up to the choice of the colors. We denote by $\mathcal{Q}'_{ij}$ the set of rooted bicolored irreducible quadrangulations with i black vertices

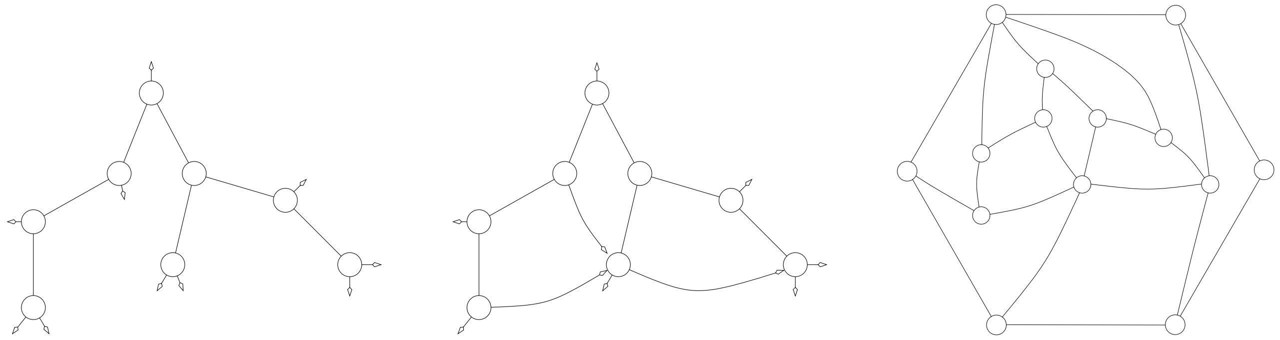

(a) A binary tree, (b) its partial closure, (c) and its complete closure.

Figure 2: The closure application.

and j white vertices and such that the root-vertex is black, and by $\mathcal{D}'_{ij}$ the set of rooted bicolored irreducible dissections with i black *inner* vertices and j white *inner* vertices and such that the root-vertex is black.

3 Closure application: from binary trees to irreducible dissections of the hexagon

3.1 Partial closure

Let T be a binary tree. Let us define a *local closure* operation based on a counter-clockwise traversal of the contour: such a traversal walks alongside the edges, in an alternating series of stems and inner edges; if a stem is followed by three inner edges, its local closure consists in merging its leaf with the extremity of the third edge, so as to create (or *close*) a quadrangular face. The involved stem is then considered as an inner edge of the obtained map, on which further local closures may be performed greedily until no more is possible. It is easy to see that the final map, called *partial closure* of T, does not depend on the order of the local closures. An example is shown in Figure 2(b).

3.2 Complete closure

We want here to complete the closure operation to obtain a dissection of the hexagon with quadrangular faces. Observe that a binary tree T with n nodes has $(n+2)$ leaves and $(n-1)$ inner edges. Hence there are $(n+2)$ stems and $(2n-2)$ sides of edges incident to the outer face at the beginning.

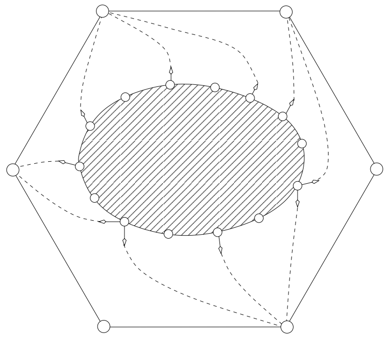

Figure 3: The end of the complete closure when $r = 2$ and $s = 2$.

As each local closure decreases by 1 the number of stems and by 2 the number of sides of inner edges which are incident to the outer face, if k denotes the number of unmatched stems in the partialclosure of T, there are $(2k-6)$ sides of inner edges incident to the outer face. Moreover, stems delimit intervals of inner edges on the contour, with length at most 2, otherwise a local closure would be possible. Let r be the number of such intervals of length 1 and s be the number of intervals of length 0 (that is, the number of nodes incident to two unmatched stems). Then r and s are clearly related by the relation $r + 2s = 6$.

The *complete closure* consists in attaching all unmatched stems to vertices of the hexagon such that each pair of consecutive stems creates a quadrangular face. As illustrated by Figure 3, there is a unique way to do this up to rotation of the hexagon. An example is given on Figure 4.

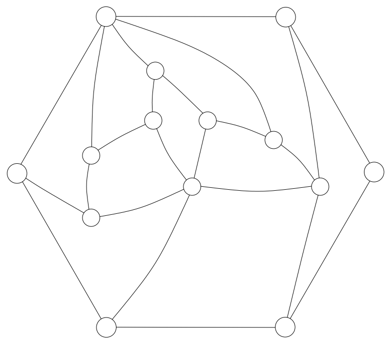

Figure 4: The complete closure of the binary tree of Figure 2(a).

Lemma 2 *The closure of a binary tree is an irreducible dissection of the hexagon.*

Proof. Suppose that, during the closure of a binary tree a, a separating 4-cycle $\mathcal{C}$ is created. As the cycle $\mathcal{C}$ is separating, there are $m \geq 1$ vertices in its interior. In addition, Euler relation and the fact that all faces in the interior of $\mathcal{C}$ have degree 4 ensure that there are $2m$ edges in the interior of $\mathcal{C}$.

Moreover we can choose a vertex v of a which will belong to the interior of $\mathcal{C}$ after the closure of a. Then we can orient the edges of a (including the buds) in the direction which goes away from v. All vertices of a have two outgoing edges for this orientation, except v, which has 3 outgoing edges. Then this orientation induces an orientation of the edges in the interior of $\mathcal{C}$ after the closure. For this induced orientation, all vertices also have outdgree 2 (in fact the vertices of the hexagon have outdegree 0 for this orientation but they can't belong to the interior of $\mathcal{C}$ as they belong to the outer face), except v which has outdegree 3. Hence there are at least $2m+1$ edges in the interior of $\mathcal{C}$, a contradiction with the counting performed at the beginning of the proof.

The same argument can be used to show that no multiple edge can be created during the closure of a binary tree.

4 Tri-orientations

4.1 Definitions

We define a kind of generalized orientation on maps, in which any edge may be non-oriented, or (*simply*) oriented in either direction, or even oriented in both directions (*bi-oriented edges*). If a map is endowed with such a generalized orientation, the *outdegree* of a vertex v is defined as the number of its incident edges that are either bi-oriented or simply oriented outward v.

The (unique) *tri-orientation* of a binary tree is defined as the generalized orientation in which inner edges are bi-oriented, and stems are simply oriented toward their leaf (see Figure 5(a) for an example). Hence each node has outdegree 3.

A *tri-orientation* of a dissection is a generalized orientation in which edges of the hexagon are not oriented and inner edges are either simply or bi-oriented in such a way that outer and inner vertices have respectively outdegree 0 and 3.

Let D be a dissection endowed with a tri-orientation. A *clockwise cycle* of D is a closed curve $\mathcal{C}$ consisting of edges of D that are either bi-oriented or simply oriented with the interior of $\mathcal{C}$ on their right.

Proposition 3

- *A tri-orientation of an element of $\mathcal{D}_n$ has $(n-1)$ bi-oriented edges and $(n+2)$ simply oriented edges.*
- *If a tri-orientation of a dissection has no clockwise cycle, then its bi-oriented edges form a spanning tree of inner vertices.*

Proof. Let $D \in \mathcal{D}_n$ endowed with a tri-orientation, and let s and r denote the respective numbers of its simply and bi-oriented edges. Euler characteristic and the degree of the faces of the dissection ensure that the dissection has $2n+1$ inner edges. Hence $2n+1 = r+s$. Moreover, as all inner vertices have outdegree 3 for the tri-orientation, $3n = 2r+s$. Hence $r = n-1$ and $s = n+2$.

The subgraph T consisting of the bi-oriented edges and their extremities has $r = n-1$ edges, no cycle (otherwise such a cycle could be traversed clockwise as all its edges are bi-oriented), and at most n vertices since outer vertices can not belong to T. Hence T is a tree that spans exactly the n inner vertices. □

4.2 Closure-tri-orientation of a closure-dissection of the hexagon.

A dissection of the hexagon that can be obtained as the closure of a binary tree will be called a *closure-*

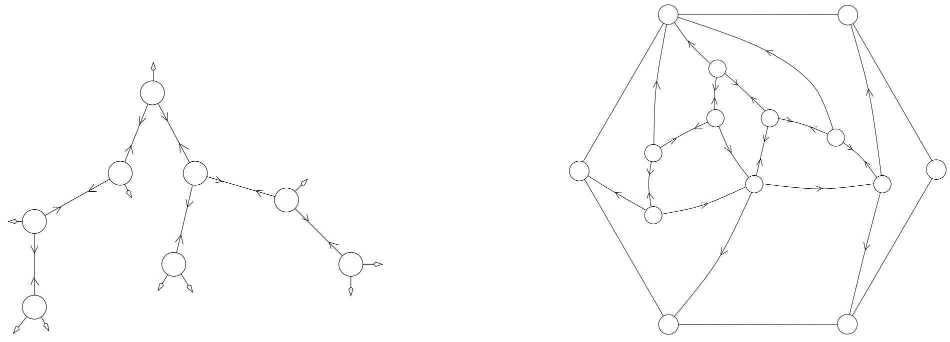

(a) A binary tree with its tri-orientation, (b) and the closure-tri-orientation of its closure.

Figure 5: Examples of tri-orientations.

dissection. Let D be such a closure-dissection, obtained by the closure of a binary tree T. The tri-orientation of T clearly induces *via* the closure operation a tri-orientation of D, called a *closure-tri-orientation*. On this tri-orientation, bi-oriented edges correspond to inner edges of the original binary tree, see Figure 5(b).

Lemma 4 *There is no clockwise cycle in a closure-tri-orientation of a closure-dissection.*

Proof. No clockwise cycle can be created during the completion of the closure (illustrated in Figure 3), since cycles created during this step involve edges of the hexagon, which are not oriented. Hence clockwise cycles may only have been created during a local closure. However such closure edges have the outer face on their right, which contradicts the orientation of the cycle. □

5 The opening application

Proposition 3 and Section 4.2 give all necessary elements to describe the inverse application of the closure, which is called the *opening application*: let D be a closure-dissection endowed with its closure-tri-orientation; then the only binary tree whose closure is D is obtained by removing edges and vertices of the hexagon and detaching all simply oriented edges at their extremity.

Actually, the general opening application of an irreducible dissection D is defined as follows:

- endow D with a tri-orientation without clockwise cycle;
- remove the vertices and edges of the hexagon;
- disconnect all simply oriented edges of the tri-orientation at their extremity.

In order for this application to be correctly defined, we need the following theorem:

Theorem 5 *Any irreducible dissection has a unique tri-orientation without clockwise cycle.*

This theorem is rather difficult to prove and will be the object of section 7.

6 Statement of the main theorem

Lemma 6 *Let $d \in \mathcal{B}_n$ be an irreducible dissection obtained by the closure of a binary tree $a \in \mathcal{B}_n$. Then the opening of d is a.*

Proof. The closure-tri-orientation of d has no clockwise cycle and Theorem 5 ensures the uniqueness of such a tri-orientation. Hence the tri-orientation of d computed at the first step of the opening algorithm is the closure-tri-orientation of d. By definition of the closure-tri-orientation, we retrieve the binary tree a whose closure is d by removing the edges and vertices of the hexagon and by disconnecting the simply oriented edges at their extremity, which is done in the second step of the opening algorithm. □

Lemma 7 *Let $a \in \mathcal{B}_n$ be a binary tree obtained by the opening of an irreducible dissection $d \in \mathcal{D}_n$. Then the closure of a is d.*

Proof. The last step of the closure application (complete closure) is clearly the inverse of the first step of the opening algorithm.

Concerning the second step of the opening algorithm, we have to give a chronological order to the simply oriented edges that we disconnect, in such a way that the inverse operation of each disconnection consists in a local closure. Hence we have to find at each step a simply oriented edge of the outer face with the outer face on its right.

At each step k we denote by m_k the subgraph of the dissection consisting of the edges which have not been removed or disconnected at their extremity. As long as not all simply oriented edges have been disconnected at their extremity, m_k has at least n edges (see Proposition 3) and its incident vertices are the n inner vertices of d. Hence it has at least a cycle, which implies that a simple closed curve c can be extracted from the contour of the outer face of m_k. At least one edge e of c is simply oriented with the interior of c on its left, otherwise c would be a clockwise cycle of the tri-orientation, which is impossible. Hence this edge e has the outer face of m_k on its right and can thus be chosen to be disconnected at its extremity.

At the end there remain just the bi-oriented edges of the tri-orientation. We know from Proposition 3 that these bi-oriented edges form a spanning tree of the inner vertices of d and are the inner edges of a binary tree a whose buds are the disconnected simply oriented edges. The chronogical order that we have chosen to perform the disconnections of simply oriented edges ensures that the partial closure of a is the figure obtained after the first step of the opening algorithm, which concludes the proof. $\square$

Theorem 8 *The closure application is a bijection between the set $\mathcal{B}_n$ of binary trees with n inner vertices and the set $\mathcal{D}_n$ of irreducible dissections with n inner vertices. The inverse of the closure application is the opening application.*

We can state two analogous versions of Theorem 8 for rooted objects:

Theorem 9
- *The application which consists in the closure of a rooted binary tree of $\mathcal{B}'_n$ and then the rooting of one of the 6 edges of the obtained dissection is a 6-to-$(n+2)$ application between $\mathcal{B}'_n$ and $\mathcal{D}'_n$.*
- *The application which consists in the closure of a rooted binary tree of $\mathcal{B}'_{ij}$ and then the rooting of one of the 3 edges of the hexagon of the obtained dissection and whose origin is a black vertex*[2] *is a 3-to-$(2i-j+1)$ application between $\mathcal{B}'_{ij}$ and $\mathcal{D}'_{i+3,j+3}$.*

Proof.
We define the set $\mathcal{D}''_n$ of so-called bi-rooted bicolored irreducible dissections of the hexagon. An object of $\mathcal{D}''_n$ is an object of $\mathcal{D}'_n$ such that, after having computed its tri-orientation without clockwise cycle, we mark one of its simply oriented edges. Then we have a surjection from $\mathcal{D}'_n$ to $\mathcal{B}'_n$ which consists in the opening of the dissection and then the rooting of the obtained binary tree at the bud corresponding to the marked edge. Each object of $\mathcal{B}'_n$ has clearly 6 preimages for this surjection (the root of the dissection could have occupied the 6 edges of the hexagon). Moreover, we can define a surjection from $\mathcal{D}''_n$ to $\mathcal{D}'_n$. It consists in erasing the mark of the marked simply oriented edge. As there are $(n+2)$ simply oriented edges in a tri-orientation, this surjection has $(n+2)$ pre-images. Hence the closure-application is a 6-to-$(n+2)$ application between $\mathcal{B}'_n$ and $\mathcal{D}'_n$.

The fact that the closure application is a 3-to-$(2i-j+1)$ application can be proved similarly. It uses in particular the fact that an object of $\mathcal{D}_{ij}$ endowed with its tri-orientation without clockwise cycle has $(2i-j+1)$ simply oriented edges whose origin is a black vertex. $\square$

Theorem 9 and the knowledge of the cardinals of $\mathcal{B}'_n$ and $\mathcal{B}'_{ij}$[3] imply the following enumerative results:

Corollary 10 $|\mathcal{D}'_n| = \frac{6}{n+2}|\mathcal{B}'_n| = \frac{6(2n)!}{(n+2)!n!}$
$|\mathcal{D}'_{ij}| = \frac{3}{2i-j+1}|\mathcal{B}'_{ij}| = \frac{3}{(2i+1)(2j+1)}\binom{2j+1}{i}\binom{2i+1}{j}$

7 Proof of Theorem 5

7.1 α-orientations

A *planar map* is a proper embedding of a connected graph in the plane. This terminology will be used in the following (it is synonimous of planar graph).

[2] More precisely, doing a traversal of the hexagon with the infinite face on our right, we choose one of the 3 edges that we reach from a black vertex and root this edge with the black vertex as origin.

[3] The cardinal of $\mathcal{B}'_n$ is well known to be the n^{th} Catalan number and the cardinal of $\mathcal{B}_{ij}$ will be found in section A.2.

Definition. In [13], Felsner introduces the notion of α-orientation. Let $G = (V, E)$ be a planar map and $\alpha : V \to \mathbb{N}$. An α-orientation of G is an orientation of the edges of G such that $\forall v \in V$, there are $\alpha(v)$ edges incident to v which are directed outward. If there exists an orientation of the edges of G which is an α-orientation, then the function α is said *feasible* in G.

Derivated map of a 3-connected map. Let G be a 3-connected planar map whose outer face is triangular. The *derivated map* G' of G is obtained by superposing G and its dual map G^* and by removing the dual vertex v_∞^* corresponding to the outer face of G. The map G (resp. G^*) is called the *primal map* (resp. the *dual map*) of G'. To each edge e of G corresponds an edge-vertex of G' of degree 4. This edge-vertex is the intersection of e and its dual edge in G^*. Moreover, we add to each of the three border vertices a_1, a_2 and a_3 of G an half-edge directed toward the infinite face. An example of a derivated map can be seen on Figure 15a where the edges of G are darker than the edges of G^*.

Theorem of Felsner. Felsner obtains in [13] the following results:

Theorem 11
- *For a planar map G and a feasible function α, there exists a unique α-orientation of G without clockwise cycle. This α-orientation is said minimal.*
- *For the derivated map of a 3-connected planar map whose outer face is triangular, the function α_0 such that $\alpha_0(v) = 3$ for all primal and dual vertices and $\alpha_0(v) = 1$ for all edge-vertices is a feasible function.*

As we can see, there exists a theorem of existence and uniqueness of an orientation without clockwise cycle of the edges of a graph such that the outdegree of each vertex is fixed. However, this theorem can not be used directly to prove Theorem 5 because there are bi-oriented edges on a tri-orientation. To use this theorem, we have to associate another map to an irreducible dissection, also called derivated map of the dissection (this will be done in section 7.3).

Actually, it is more practical to define a derivated map for so-called bicolored complete irreducible dissections, which form a subset of the irreducible dissections. Hence we will work only with this subset and thus we have first to prove in section 7.2 that Theorem 5 is true if we can prove the uniqueness and existence of a tri-orientation without clockwise cycle for this subset of irreducible dissections.

Then we will prove that a tri-orientation without clockwise cycle of a dissection can be transposed injectively in an α_0-orientation without clockwise cycle of its derivated map. By injectivity of the transposition and by uniqueness of the α_0-orientation without clockwise cycle, this will imply the uniqueness of a tri-orientation without clockwise cycle. Reciprocally, we have to prove that an α_0-orientation without clockwise cycle of the derivated map can be transposed in a tri-orientation without clockwise cycle of its associated dissection. This will imply the existence of a tri-orientation without clockwise cycle and conclude the proof of Theorem 5.

7.2 Complete bicolored irreducible dissections

Introduction. In this subsection we define a subset of irreducible dissections, called bicolored complete irreducible dissections. Then the object of the section is to show that, to prove Theorem 5, it suffices to prove the uniqueness and existence of a so called complete-tri-orientation without clockwise cycle for each bicolored complete irreducible dissection.

Definition. A bicolored irreducible dissection is said *complete* if the three white vertices of the hexagon have two incident edges. Hence these two edges are the two edges of the hexagon that are incident to the border vertex.

Completion of a bicolored irreducible dissection. For any bicolored irreducible dissection d, we define its completed dissection d^c as follows . For each white vertex v of the hexagon, we denote by e_1 and e_2 the two edges of the hexagon which are incident to v and we denote by v_1 and v_2 the respective extremities of e_1 and e_2. If v has at least 3 incident edges in the dissection, then we create a new white vertex v' outside of the hexagon and we link v' to v_1 and to v_2 by two new edges e'_1 and e'_2, see Figure 6.

At the end, the obtained dissection is a bicolored dissection of the hexagon such that the three white vertices of the hexagon have two incident edges, see the transition between Figure 7a and Figure 7b (ignore here the orientation of edges on this figure).

Lemma 12 *The completed bicolored dissection d^c of an irreducible dissection d is a bicolored complete irreducible dissection.*

Proof. The dissection d^c is complete by construction. Hence, we just have to prove that d^c is irreducible. As d is irreducible, if a separating 4-cycle $\mathcal{C}$ appears in d^c when the completion is performed, then it must contain a white vertex v' of the hexagon of d^c such that v' has been added during the completion. Hence, using the notations of the definition of the completion, two edges of $\mathcal{C}$ are the edges e_1' and e_2' incident to v' in d^c. The two other edges e_1'' and e_2'' of $\mathcal{C}$ form a path of length 2 which connects the extremities v_1 and v_2 of e_1' and e_2' and passes by the interior of d (otherwise the separating 4-cycle $\mathcal{C}$ would consist in the edges e_1', e_2', e_1 and e_2 and then it would delimit a face). As d is irreducible, the 4-cycle $\mathcal{C}'$ of d consisting of the edges e_1, e_2, e_1'' and e_2'' delimits a face. Hence e_1 and e_2 are incident to the same inner face of d, which implies that the white vertex v of the hexagon of d associated to v' has degree 2. But, by definition of the completion, the creation of a new vertex v' associated to v is performed only if v has at least 3 incident edges. Hence we have a contradiction. □

Tri-orientations. Let d be a bicolored irreducible dissection and let d^c be its completed bicolored dissection. Then we define an application Φ from the tri-orientations of d^c to the tri-orientations of d. Given a tri-orientation t of d^c, we remove the edges which have been added to obtain d^c from d, we erase the orientation of the edges of the hexagon which are inner edges of d^c. We obtain thus a tri-orientation of d that we denote by $\Phi(t)$, see the transition between Figure 7b and Figure 7a.

Lemma 13
- *If $\tilde{t}$ is a tri-orientation of d^c without clockwise cycle, then the tri-orientation $\Phi(\tilde{t})$ of d has no clockwise cycle.*
- *For each tri-orientation t of d without clockwise cycle, there exists a tri-orientation $\tilde{t}$ of d^c without clockwise cycle such that $\Phi(\tilde{t}) = t$.*

Proof. The first point is trivial as the tri-orientation $\Phi(\tilde{t})$ is just obtained by removing some edges and some orientations of edges.

For the second point, the preimage $\tilde{t}$ is constructed as follows. Consider each white vertex v of the hexagon of d which has degree at least 3. Let $(e_1, \ldots, e_m)$ $(m \geq 3)$ be the series of edges incident to v in d in the counter-clockwise order around v such that e_1 and e_2 are the two edges of the hexagon that are incident to v (we note v_1 and v_2 their respective extremities). As $m \geq 3$, the vertex v gives rise to a new vertex v' with two incident edges e_1' and e_2' such that the edges e_1, e_2, e_1' and e_2' form a new face f. Then the edges e_1 and e_2 become internal edges of d^c and have thus to be oriented. As their respective extremities v_1 and v_2 are vertices of the hexagon of d^c, e_1 and e_2 have to be oriented respectively toward v_1 and v_2. Then the vertex v has degree 2 after these two orientations and we have to give to v a third outgoing edge.

We thus have the choice to bi-orient one of the edges $e_3, \ldots, e_m$. The judicious choice to avoid the appearance of a clockwise cycle is to bi-orient e_3, see Figure 6. Indeed, if these new orientations of edges have created a simple clockwise cycle $\mathcal{C}$, then the cycle must pass by v. It arrives at v by one of the edges e_{i_0} with $4 \leq i_0 \leq m$ directed toward v. Moreover it must go outward of v using the edge e_3. Indeed the two other outgoing edges e_1 and e_2 of v have an extremity which is on the border of the hexagon and thus has outdegree 0. Hence the interior of the simple cycle $\mathcal{C}$ must contain all incident faces of v which are on the right of v when we traverse v from e_{i_0} and go out using e_3. Hence the interior of $\mathcal{C}$ must contain the new face f of d^c. But f is on the border of the hexagon, hence a cycle $\mathcal{C}$ containing f must pass by the edges of f which are on the border of the dissection d^c. As these edges are not oriented by definition of a tri-orientation, we have a contradiction. Hence we have constructed a tri-orientation $\tilde{t}$ of d^c without clockwise cycle and such that $\Phi(\tilde{t}) = t$. An example of this construction can be seen as the transition between Figure 7a and Figure 7b. □

Proposition 14
- *The existence of a tri-orientation without clockwise cycle for any bicolored complete irreducible dissection implies the existence*

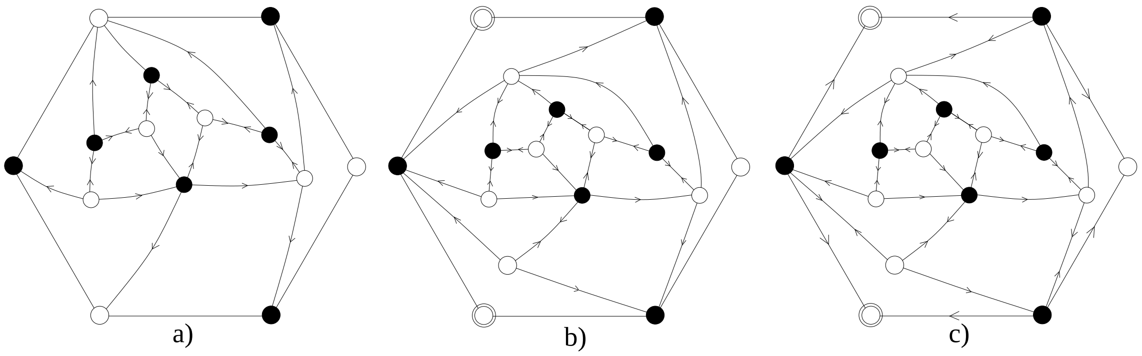

Figure 7: An irreducible dissection d with a tri-orientation t without clockwise cycle endowed with a bicoloration on Figure a. Its associated completed dissection d^c with a tri-orientation $\tilde{t}$ without clockwise and preimage of t by Φ (Figure b). The dissection d^c with a complete-tri-orientation without clockwise cycle and preimage of $\tilde{t}$ by Ψ (Figure c).

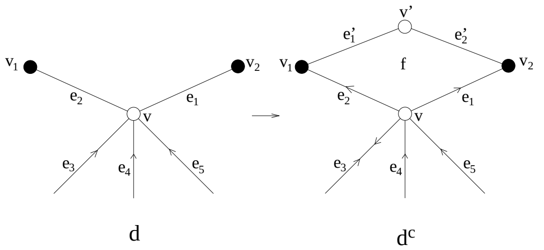

Figure 6: From a tri-orientation t of d without clockwise cycle, the rules of construction of a tri-orientation $\tilde{t}$ of d^c without clockwise cycle.

of a tri-orientation without clockwise cycle for any irreducible dissection.

- *The uniqueness of a tri-orientation without clockwise cycle fo any bicolored complete irreducible dissection implies the uniqueness of a tri-orientation without clockwise cycle for any irreducible dissection.*

Proof. This proposition is a clear consequence of Lemma 12 and Lemma 13. □

Complete-tri-orientations. A complete-tri-orientation of a bicolored complete irreducible dissection d is an orientation of the edges of d which is defined as follows. Each edge e, even the edges of the hexagon, is either simply oriented or bi-oriented with the two half-edges of e directed outward of their respective origin. In addition each inner vertex of d and the 3 black vertices of the hexagon of d have outdegree 3. Finally the 3 white vertices of the hexagon of d have outdegree 0.

Lemma 15 *Let $d \in \mathcal{D}_n$ be a bicolored complete irreducible dissection endowed with a complete-tri-orientation without clockwise cycle. Then the subgraph A of d consisting of the bi-oriented edges of d is a tree incident to all vertices of d except the three white vertices of the hexagon of d.*

Proof. We reason similarly as in Proposition 3. We denote by r and s the respective number of bi-oriented and simply oriented edges of $\tilde{d}$. From Euler relation and the degrees of the faces of d, there are $2n+7$ edges in d, hence $r+s = 2n+7$. In addition, the n inner vertices and the three black (resp. white) vertices of the hexagon of d have outdegree 3 (resp. 0). Hence $2r + s = 3(n + 3)$. Thus, $r = n+2$ and $s = n+5$. Hence the subgraph A has $n+2$ edges, has no cycle (otherwise, it would imply a clockwise cycle on d), and is incident to at most $(n + 3)$ vertices, which are the inner vertices and the three black vertices of the hexagon of d. Finally, a classical result of graph theory ensures that A is a tree incident to all these $(n+3)$ vertices. □

Lemma 16 *Let $d \in \mathcal{D}_n$ be a bicolored complete irreducible dissection endowed with a tri-orientation t without clockwise cycle. Then, for each black vertex v of the hexagon, two of its outgoing incident edges are its two incident edges which belong to the hexagon and are simply oriented. Moreover its third outgoing edge is bi-oriented.*

Proof. The fact that the two edges of the hexagon incident to v are simply oriented outward of v follows from the fact that the three white vertices of the hexagon have outdegree 0. The second assertion is a consequence from the fact that the subgraph A consisting of the bi-oriented edges of d forms a tree incident to all vertices of d except the three white vertices of the hexagon of d. Hence there is a bi-oriented edge e incident to each black vertex v of the hexagon and this edge consitutes the third outgoing edge of v. □

Let d be a bicolored complete irreducible dissection. Then we define an application Ψ from the complete-tri-orientations without clockwise cycle of d to the tri-orientations of d, defined as follows. Let t be a complete-tri-orientation without clockwise cycle. To obtain $\Psi(t)$, we erase first the orientation of the edges of the hexagon of d. Then, for each black vertex v of the hexagon of d, we orient the unique outgoing inner edge e of v toward v. As e is bi-oriented according to Lemma 16, the change of orientation of e doesn't increment the outdegree of the vertex v' connected to v by e, hence the outdegree of v' remains 3. Finally the obtained orientation $\Psi(t)$ of d is a tri-orientation.

Lemma 17 *Let d be a bicolored complete irreducible dissection.*

- *If $\tilde{t}$ is a complete-tri-orientation of d without clockwise cycle, then the tri-orientation $\Psi(\tilde{t})$ of d has no clockwise cycle.*
- *For each tri-orientation t of d without clockwise cycle, there exists a complete-tri-orientation $\tilde{t}$ of d without clockwise cycle such that $\Psi(\tilde{t}) = t$.*

Proof. The first point is trivial. For the second point, we reason similarly as in Lemma 13: for each black vertex v of the hexagon of d, let $(e_1, \ldots, e_m)$ $(m \geq 3)$ be the series of edges incident to v in d in the counter-clockwise order around v such that e_1 and e_2 are the two edges of the hexagon that are incident to v. Then we bi-orient e_3, which is the "leftmost" inner edge of v. An argument similar as in the proof of the second point of Lemma 13 ensures that this choice is judicious to avoid the creation of a clockwise cycle passing by v when we bi-orient this edge. An example of this construction can be seen as the transition between Figure 7b and Figure 7c. □

Proposition 18

- *The existence of a complete-tri-orientation without clockwise cycle for any bicolored complete irreducible dissection implies the existence of a tri-orientation without clockwise cycle for any irreducible dissection.*
- *The uniqueness of a complete-tri-orientation without clockwise cycle for any bicolored complete irreducible dissection implies the uniqueness of a tri-orientation without clockwise cycle for any irreducible dissection.*

Proof. This proposition is a clear consequence of Lemma 17 and Proposition 14. □

As a consequence, to prove Theorem 5, we just have to prove the existence and uniqueness of a complete-tri-orientation without clockwise cycle for each complete bicolored irreducible dissections. To prove Theorem 5, we will work with this subset of the irreducible dieesctions.

7.3 Derivated map of a bicolored complete irreducible dissection

The *derivated map* G' of a bicolored complete irreducible dissection d is constructed as follows.

The edges of the derivated map are obtained in the following way: for each inner face f of the dissection, link the two black vertices incident to the face by an edge called a *primal edge* and link the two white vertices incident to the face by an edge called a *dual edge*. These two edges (which are the two diagonals of f) intersect in a new vertex v_f of the derivated map called an *edge-vertex*, see Figure 8 (ignore the orientation of the edges until Section 7.4).

The black vertices are called *primal vertices* of the derivated map and the white vertices are called *dual vertices* of the derivated map. The submap G (resp G^*) of the derivated map consisting of the primal (resp. dual) vertices and the primal (resp. dual) edges is called the *primal map* (resp. the *dual map*) of the derivated map.

Definition. A planar map is said 3-connected if it has no multiple edges and at least 3 vertices must be removed to disconnect the map.

Lemma 19 *The primal map G of the derivated map of a bicolored complete irreducible dissection is a 3-connected planar map whose outer face is triangular.*

Proof. The fact that the outer face of G is triangular follows from the fact that all white vertices of the hexagon of a bicolored complete irreducible dissection are incident to a unique inner face. Suppose that there exists two vertices v_1 and v_2 of G such that the removal of v_1 and v_2 disconnects G. Then there exists a simple closed curve $\mathcal{C}$ which passes by v_1 and v_2, which does not pass by any other vertex or cut any edge of G, and such that there exists at least one vertex of G in the interior and in the exterior of $\mathcal{C}$. The vertices v_1 and v_2 cut $\mathcal{C}$ in two paths p_1 and p_2. As $\mathcal{C}$ doesn't cut any edge or vertex on p_1 and p_2, the paths p_1 and p_2 are respectively included in two faces f_1 and f_2 of G. By construction of the derivated map, the map G^* is the classical dual map of G. Hence there exists two dual (white) vertices v_{f_1} and v_{f_2} in the interior of f_1 and f_2. Hence we can deform homotopically the curve $\mathcal{C}$ so that it goes from v_1 to v_{f_1} and from v_{f_1} to v_2 using two edges of the original irreducible dissection d, and similarly goes from v_2 to v_{f_2} and from v_{f_2} to v_1 using two edges of the original irreducible dissection d. Hence we can deform $\mathcal{C}$ so that it delimits a separating 4-cycle of d, which is impossible by irreducibility of d. □

7.4 Transposition rules for orientations

We can associate to a complete-tri-orientation of a bicolored complete irreducible dissection d an orientation of the edges of the derivated map G' of d in the following way.

Let v be a vertex and let e be an inner edge of the dissection such that e is incident to v. Let e' be the edge of the derivated map[4] which succeeds e in the counter-clockwise order around v. If e is directed outward of v (i.e. bi-oriented or simply oriented outward) then we orient e' outward of v. Otherwise we orient e' toward v. The application of the local rules are illustrated on Figure 8.

Lemma 20 *Let $d \in \mathcal{D}_n$ be a bicolored complete irreducible dissection endowed with a complete-tri-orientation without clockwise cycle. Then the orientation of edges of the derivated map G' of d obtained by the transposition rules has the following properties:*

- *Each primal or dual vertex of G' has outdegree 3.*
- *Each edge-vertex of G' has outdegree 1.*

Hence, using the notation of Section 7.1, the orientation of edges of G' obtained by the transposition rules is an α_0-orientation.

Proof. The first point is trivial.

For the second point, let f be an inner face of d and v_f the associated edge-vertex in G' (we recall that v_f is the intersection of the two diagonals of f). Doing a clockwise traversal of the contour of f, for each edge e of f, we denote by v_e the vertex from which we reach e. From the transposition rules for orientations, we know that the edge e' linking v_e and v_f in G' is outgoing of v_f iff e is simply oriented toward v_e.

Hence, to establish the second point, we have to prove that for each inner face f of d, the number n_f of edges of f which are simply oriented in the counter-clockwise direction around f is equal to 1. First we have $n_f \geq 1$, otherwise the contour of f would be a clockwise cycle in the complete-tri-orientation, which is impossible. Using Euler relation and the degrees of the faces of d, it is easy to prove that if d has n inner vertices, then it has $(n+2)$ inner faces. Let $\tilde{s}$ be the number of simply oriented edges of d which have an inner face of d on their left. Clearly $\tilde{s}+3$ is the number of simply oriented edges of d as only three simply oriented edges have the infinite face on their left (see Figure 7c). Hence, from Lemma 15, $\tilde{s}+3 = n+5$, thus $\tilde{s} = n+2$. Moreover $\tilde{s}$ is clearly equal to $\sum_f n_f$. Finally the pigeonhole's principle ensures that $n_f = 1$ for all inner faces, which ensures that all edge-vertices have outdegree 1 after having performed the transposition rules for orientation. □

7.5 Uniqueness of a tri-orientation without clockwise cycle

The following lemma completes Lemma 20 and is crucial to establish the uniqueness of a tri-orientation without clockwise cycle for any irreducible dissection.

[4] Recall that an edge of the derivated map corresponds to an half-edge of the primal map or to an half-edge of the dual map, hence it connects a primal or dual vertex and an edge-vertex.

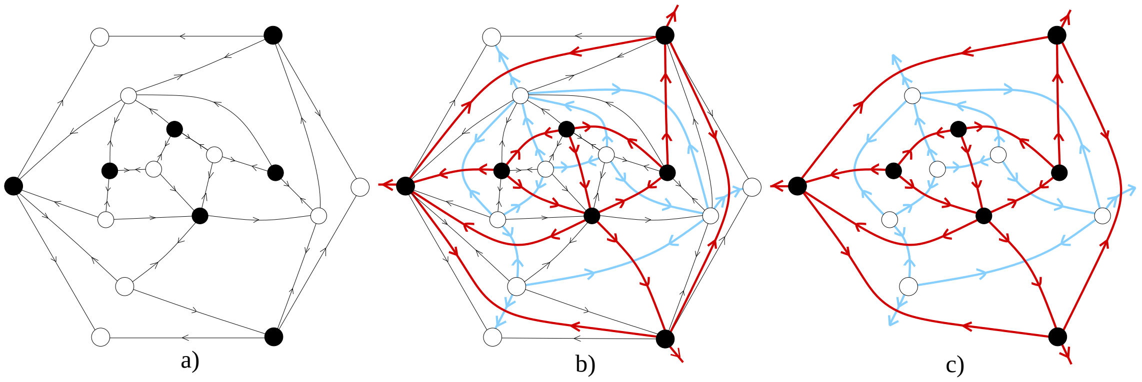

Figure 8: The construction of the derivated map of a bicolored complete irreducible dissection. The application of the transposition rules on a complete-tri-orientation without clockwise cycle of the dissection.

Lemma 21 *Let d be a bicolored complete irreducible dissection endowed with a complete-tri-orientation t without clockwise cycle. Let G' be the derivated map of d. Then the α_0-orientation X of G' obtained from t by the transposition rules has no clockwise cycle.*

Proof. Suppose that X has a clockwise cycle $\mathcal{C}$. Each edge of G' connects an edge-vertex and a vertex of the original dissection d. Hence the cycle $\mathcal{C}$ consists of a sequence of couples $(\underline{e}, \overline{e})$ of consecutive edges of G' such that $\underline{e}$ goes from a vertex $\underline{v}$ of the dissection toward an edge-vertex v' of G' and $\overline{e}$ goes from v' toward a vertex $\overline{v}$ of the dissection. Let $(e'_1, \ldots, e'_m)$ be the sequence of edges of G' incident to v' and between $\underline{e}$ and $\overline{e}$ in the clockwise order around v', so that $e'_1 = \underline{e}$ and $e'_m = \overline{e}$ and let $(v_1, \ldots, v_m)$ be their respective extremities, so that $v_1 = \underline{v}$ and $v_m = \overline{v}$. Note that $2 \leq m \leq 4$.

As each edge-vertex has outdegree 1 in X and as e'_m is going out of v', the edges $e'_1, \ldots, e'_{m-1}$ are directed toward v'. Hence the transposition rules for orientations ensure that the edges (v_i, v_{i+1}), for $1 \leq i \leq m-1$, are all bi-oriented or oriented from v_i to v_{i+1} in the complete-tri-orientation t of d. Hence we can go from $\underline{v}$ to $\overline{v}$ passing by the exterior of $\mathcal{C}$ and using only edges of d, see Figure 9 for an example, where $m = 3$.

Concatenating the paths of edges of d associated to each couple $(\underline{e}, \overline{e})$ of $\mathcal{C}$, we obtain an oriented path of d enclosing the interior of $\mathcal{C}$ on its right. Then a simple clockwise cycle can be extracted from this closed path, see Figure 10. As the complete-tri-orientation t has no clockwise cycle, this gives a contradiction. □

□

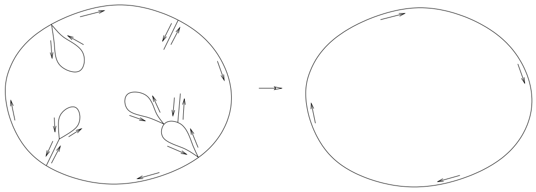

Figure 10: A simple clockwise cycle can be extracted from an oriented path of a tri-orientation enclosing a bounded region on its right.

Proposition 22 *Each irreducible dissection has at most one tri-orientation without clockwise cycle.*

Proof. Let d be a bicolored complete irreducible dissection and G' its derivated map. A first important remark is that the transposition rules define an injective application. In addition, Lemma 21 ensures that the image of any tri-orientation of d without clockwise cycle is an α_0-orientation of G' without clockwise cycle. Hence the injectivity of the application and the uniqueness of an α_0-orientation without clockwise cycle in G' (see Theorem 11) ensure that d has at most one tri-orientation without clockwise cycle. Finally, Proposition 18 ensures that any irreducible dissection has at most one tri-orientation without clockwise cycle.
□

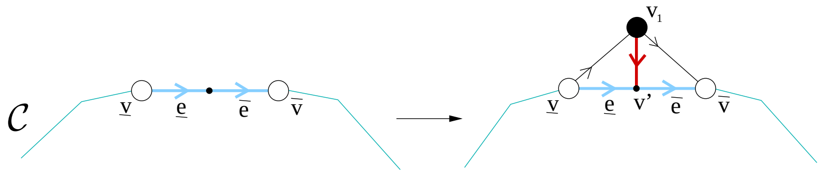

Figure 9: An oriented path of edges of the dissection can be associated to each couple $(\underline{e}, \overline{e})$ of consecutive edges of $\mathcal{C}$ such that the origin of $\underline{e}$ is a vertex of the dissection.

7.6 Existence of a tri-orientation without clockwise cycle

Inverse of the transposition rules. Let d be a bicolored complete irreducible dissection and G' its derivated map. Given an α_0-orientation of G' we can associate to this orientation an orientation of the half-edges of d by performing the inverse of the transposition rules. Hence, for each half-edge h of d, we note v_h its origin and we orient h like the edge e' of G' that succeeds h in the clockwise order around v_h, see Figure 8b.

The inverse of the transposition rules is clearly such that a vertex has the same outdegree in the obtained orientation of edges of d as on the α_0-orientation of G'. Hence each inner vertex of d has outdegree 3 and each white (resp. black) vertex on the hexagon of d has outdegree 0 (resp. 3). Then, for any edge e of d, if the two half-edges of e have the same direction for the obtained orientation, then we simply orient e in the direction of its two half-edges. Otherwise the two half-edges of e have an opposite direction and two cases can arise: either the two half edges of e are directed outward of their respective origin, or they are directed toward their respective origin. This last case is incompatible with the definition of a tri-orientation. However, as the edge-vertices have outdegree 1 in an α_0 orientation of G', this case implies that the contour of the face f_e of G' associated to e is a clockwise cycle, see Figure 11.

Hence, if G' is endowed with its α_0-orientation without clockwise cycle, the orientation of edges of d obtained by the inverse of the transposition rules is a complete-tri-orientation.

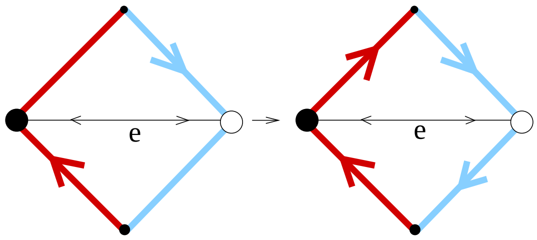

Figure 11: The case where the two half-edges of e are oriented toward their origin implies that the contour of the associated face of G' is a clockwise cycle.

Turnright-most paths. In view of Lemma 24, we define particular paths of edges on the derivated map G' endowed with an α_0-orientation, called *turnright-most paths*. A turnright-most path P of G' is an oriented path of G', i.e. a sequence of vertices $(v_0, \ldots, v_m)$ such that two consecutive vertices v_i and v_{i+1} are connected by an edge e_i of G' oriented from v_i to v_{i+1}. In addition, the first vertex v_0 of P must be a primal or dual vertex of G', i.e. a vertex of the bicolored complete irreducible dissection d associated to G'. Finally, for each primal or dual vertex v_i of P different from the first and last vertex of P [5], there is no outgoing edge of v_i between e_{i-1} and e_i if we turn around v_i in the counter-clockwise order. This property explains why we call these paths turnright-most paths.

Lemma 23 *No simple counter-clockwise cycle can be extracted from a turnright-most path.*

Proof. Suppose that a simple counter-clockwise cycle $\mathcal{C}$ can be extracted from a turnright-most path P of a derivated map G'. We denote by B the interior of $\mathcal{C}$. The cycle $\mathcal{C}$ is closed when the path P returns at index j_0 to a vertex by which P has already passed at a step $i_0 < j_0$, so that $v_{i_0} = v_{j_0}$. Moreover, as $\mathcal{C}$ is a simple closed curve, all vertices v_i with $i_0 \leq i < j_0$ are distinct. In addition, as P is turnright-most and as $\mathcal{C}$ is a counter-clockwise

[5] As v_0 is a primal or dual vertex and as an edge of the derivated map always connects an edge-vertex and a primal or dual vertex, the primal or dual vertices are the v_i whose index i is an even number.

cycle, each vertex v_i with $i_0 < i < j_0$ has an outgoing edge used by P to go out of v_i and has its two other outgoing edges in B.

Let m be the submap obtained from G' by removing the edges and vertices outside of $\mathcal{C}$. We are going to prove that the conjonction of all incidence relations on m makes it impossible that a counter-clockwise cycle $\mathcal{C}$ is created. In this purpose, we have to introduce several parameters associated to m. Let n_v be the number of primal vertices of m and n_f be the number of dual vertices of m. Let $n_e^{(int)}$ be the number of inner edge-vertices of m. Let $n_e^{(2)}$, $n_e^{(3)}$ and $n_e^{(4)}$ be the numbers of edge-vertices on the border of m which have respectively 2, 3 and 4 incident edges in m. We define the quantity b as $b = 2n_e^{(2)} + 3n_e^{(3)} + 4n_e^{(4)}$. We also define the quantity k as $k = n_e^{(2)} + n_e^{(3)} + n_e^{(4)}$, hence k corresponds to the number of edge-vertices on the border of m and $2k$ corresponds to the number of edges on the border of m. Finally, let e be the number of edges of m and f be the number of inner faces of m.

First the Euler relation on m is $(n_v+n_f+n_e^{(int)}+k)+f = e+1$. Moreover, all inner faces have degree 4 and there are $2k$ edges on the border of m, hence $4f = 2e - 2k$. In addition, counting the edges of m according to the degree of all edge-vertices of m gives $e = 4n_e^{(int)}+b$. Using these two last equalities, Euler relation becomes $n_v+n_f+\frac{1}{2}k = n_e^{(int)}+\frac{1}{2}b+1$. The edges of m can also be counted according to their origin in the α_0-orientation. As already said, the 3 outgoing edges of the border vertices v_i, with $i_0 < i < j_0$, belong to m. Clearly, all edge-vertices of m also have their unique outgoing edge belonging to m and all inner primal or dual vertices have their 3 outgoing edges in m. Hence all primal or dual vertices except perhaps v_{i_0} have their 3 outgoing edges belonging to m. Finally, noting $1 \leq d_{i_0} \leq 3$ the outdegree of v_{i_0} in m, we have $e = 3n_v + 3n_f + (d_{i_0} - 3) + n_e^{(int)} + k$. Hence, using Euler relation, $e = 4n_e^{(int)} - \frac{1}{2}k + \frac{3}{2}b + d_{i_0}$. As we also have obtained $e = 4n_e^{(int)} + b$, we finally obtain $\frac{1}{2}b + d_{i_0} = \frac{1}{2}k$, which is impossible because $b \geq 2k$ and $d_{i_0} \geq 1$. $\square$

Proof of existence.

Lemma 24 *Let d be a bicolored complete irreducible dissection and let G' be its derivated map, endowed with its minimal α_0-orientation that we denote by X. Let t be the complete-tri-orientation obtained from X by application of the inverse of the transposition rules. Then t has no clockwise cycle.*

Proof. Suppose that t has a clockwise cycle $\mathcal{C}$. Let $(v_1, \ldots, v_m)$ be the sequence of vertices of $\mathcal{C}$, chosing an arbitrary vertex v_1 on $\mathcal{C}$ to start, and traversing $\mathcal{C}$ in the counter-clockwise order.

Each edge (v_i, v_{i+1}) is bi-oriented or oriented with the interior of $\mathcal{C}$ on its right. Hence the edge e_i' of G' that succeeds (v_i, v_{i+1}) in the clockwise order around v_i is going out of v_i.

Let $\mathcal{P}_1$ be the turnright-most path of G' starting at e_1'. Lemma 23 ensures that a closed curve formed by $\mathcal{P}_1$ would be a clockwise cycle of X, which is impossible. Hence $\mathcal{P}_1$ doesn't pass twice by the same vertex. As the number of vertices of G' is finite, $\mathcal{P}_1$ must end at one of the 6 half-edges of the border of G' directed toward the infinite face. Hence, to reach the infinite face of G', $\mathcal{P}_1$ must reach the cycle $\mathcal{C}$ at a vertex v_{i_1}. We denote by $\widetilde{\mathcal{P}_1}$ the part of $\mathcal{P}_1$ between v_1 and v_{i_1}. Then we go out of v_{i_1} using the turnright-most path $\mathcal{P}_{i_1}$ starting at the edge e_{i_1}'. The crucial point is that the oriented path obtained by concatenating $\widetilde{\mathcal{P}_1}$ and $\mathcal{P}_{i_1}$ has the exterior of $\mathcal{C}$ on its left when it passes by v_{i_1}, see Figure 12. Hence, if we note c_1 the part of $\mathcal{C}$ such that the concatenation, noted $\mathcal{C}_1$, of c_1 and $\mathcal{P}_1$ is a clockwise cycle, then $\mathcal{P}_1$ starts in the interior of $\mathcal{C}_1$.

Similarly as $\mathcal{P}_1$, $\mathcal{P}_{i_1}$ must reach the infinite face of G', hence it must reach $\mathcal{C}_1$. Suppose that $\mathcal{P}_{i_1}$ reaches $\mathcal{C}_1$ at a vertex v belonging to $\widetilde{\mathcal{P}_1}$. Then the concatenation of the part of $\widetilde{\mathcal{P}_1}$ between v and v_{i_1} and of the part of $\mathcal{P}_{i_1}$ before v is a clockwise cycle of X, which is impossible.

Otherwise it reaches $\mathcal{C}_1$ at a vertex v_{i_2} of c_1 and not belonging to $\widetilde{\mathcal{P}_1}$. Similarly, we denote by $\widetilde{\mathcal{P}_{i_1}}$ the part of $\mathcal{P}_{i_1}$ between v_{i_1} and v_{i_2}. We also denote by $c_2 \subset c_1$ the part of $\mathcal{C}$ such that the cycle, noted $\mathcal{C}_2$, formed by c_2, $\widetilde{\mathcal{P}_1}$ and $\widetilde{\mathcal{P}_{i_1}}$ is clockwise.

We can generalise this argument and these notations for each step k. As the part c_k of $\mathcal{C}_k$ shrinks strictly at each step, there must be a step k where $\mathcal{P}_{i_k}$ meets a vertex of $\mathcal{C}_k$ belonging to $\widetilde{\mathcal{P}_1} \cup \widetilde{\mathcal{P}_{i_1}} \cup \ldots \cup \widetilde{\mathcal{P}_{i_{k-1}}}$, forming thus a clockwise cycle, see Figure 12. Finally, we have proved that the presence

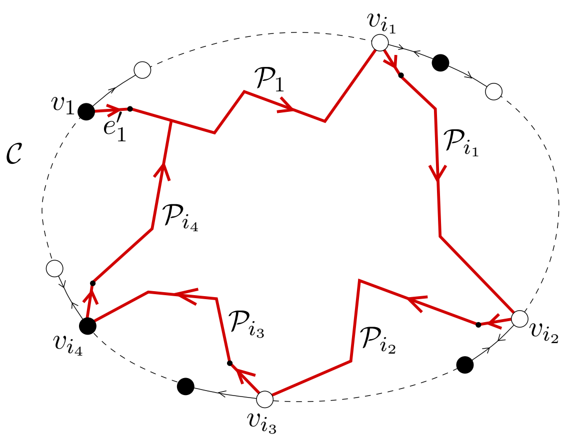

Figure 12: The presence of a clockwise cycle on t yields the presence of a clockwise cycle on X.

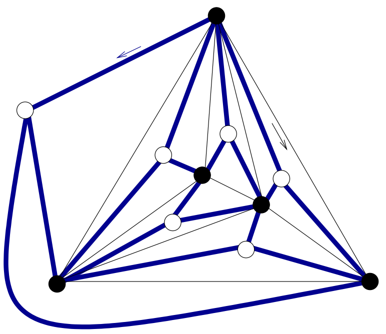

Figure 13: A rooted 3-connected planar map superposed with its associated rooted irreducible quadrangulation (with bold edges).

of a clockwise cycle on t yields the presence of a clockwise cycle on X. $\square$

As there exists an α_0-orientation without clockwise cycle for the derivated map G' (see Theorem 11), Lemma 24 ensures that there exists a complete-tri-orientation without clockwise cycle for each bicolored complete irreducible dissection. Then Proposition 18 ensures that there exists a tri-orientation without clockwise cycle for each irreducible dissection. This assertion, together with Proposition 22, concludes the proof of Theorem 5.

8 Enumerating 3-connected maps

8.1 Bijection between 3-connected maps and irreducible quadrangulations

There is a well known application between $\mathcal{Q}'_n$ and $\mathcal{P}'_n$ (resp. between $\mathcal{Q}'_{ij}$ and $\mathcal{P}'_{ij}$). Given a rooted quadrangulation $q \in \mathcal{Q}'_n$ endowed with its bicoloration of vertices, we obtain a rooted map m by linking, for each face f of q (even the outer face), the two diagonally opposed black vertices of f. Finally the root of m is chosen to be the edge corresponding to the outer face of q and whose origin is the origin of the root of q, see Figure 13.

This application is easily inversible. Given a rooted map m, it consists in adding a vertex called a face-vertex in each face (even the infinite face) of m and linking a vertex v and a face-vertex v_f by an edge if v is incident to the face f corresponding to v_f. By keeping only the edges of incidence face-vertex, we obtain a quadrangulation. We choose the root as the edge which follows the root of m in the counter-clockwise order around the origin of the root of m.

The following theorem is a classical result in the theory of maps.

Theorem 25 *The application of Tutte is a bijection between $\mathcal{P}'_n$ and $\mathcal{Q}'_n$ and a bijection between $\mathcal{P}'_{ij}$ and $\mathcal{Q}'_{ij}$.*

8.2 Definition of an injection Γ from $\mathcal{Q}'$ to $\mathcal{D}'$

We can easily associate to a rooted irreducible quadrangulation q a rooted dissection d of the hexagon in the following way: remove the root-edge of q (the outer face becomes thus hexagonal) and carry the root on the edge of the hexagon that has the same origin as the origin of the root of q and the infinite face on its right.

It is easy to see that d is an irreducible dissection of the hexagon. Indeed the presence of a separating 4-cycle in d would clearly imply the presence of a separating 4-cycle in the quadrangulation q from which we have removed the root edge.

Moreover it is trivial that this application is an injection. More precisely, it is an injection from $\mathcal{Q}'_n$ to $\mathcal{D}'_{n-4}$, [6] and it is an injection from $\mathcal{Q}'_{ij}$ to $\mathcal{P}'_{ij}$.

[6]It is easy to show, using Euler relation and the fact that all inner faces have degree 4, that an element of $\mathcal{D}_n$ has $(n+2)$ inner faces.

8.3 Decomposition of a rooted irreducible dissection

Decomposition paths. Let d be a rooted irreducible dissection. We denote by s the origin of the root and by t the vertex which is diametrically opposed to s in the outer face of d.

A path of length 3 connecting s and t is called a *decomposition path* of d. The path of 3 edges of the hexagon going from s to t with the infinite face on its right (resp. on its left) is called the left border path (resp the right border path) of d. A decomposition path different from the left border path and from the right border path is called an *inner decomposition path* of d.

Undecomposable dissections. A rooted irreducible dissection without inner decomposition path is said *undecomposable*. The respective sets of rooted irreducible undecomposable dissections with n inner vertices (resp. whose canonical bicoloration of vertices has i black vertices and j white vertices) is denoted by $\mathcal{U}'_n$ (resp. $\mathcal{U}'_{ij}$). The set of rooted irreducible undecomposable dissections is denoted by $\mathcal{U}'$.

Lemma 26 *The image of $\mathcal{Q}'_n$ (resp. of $\mathcal{Q}'_{ij}$) by the injection of Section 8.2 is $\mathcal{U}'_{n-4}$ (resp. $\mathcal{U}'_{ij}$).*

Proof. Let q be a rooted irreducible dissection and let e be the root edge of q. Let $d \in \mathcal{D}'$ be the image of q by the injection of Section 8.2, i.e. d is obtained by removing e and carrying the root on the border edge of d having the same origin as e.

Suppose that d has an inner decomposition path $\mathcal{P}$. Then the concatenation $\mathcal{C}$ of $\mathcal{P}$ and e is a 4-cycle of q. As $\mathcal{P}$ is not the left border path of d, the interior of $\mathcal{C}$ is not a face of d. As $\mathcal{P}$ is not the right border path of d, $\mathcal{C}$ is not the contour of the outer face of q. Hence $\mathcal{C}$ is a separating 4-cycle of q, in contradiction with the irreducibility of q.

Hence the image of a rooted irreducible quadrangulation by the injection is a rooted irreducible undecomposable dissection.

Reciprocally, let d be a rooted irreducible undecomposable dissection. Let q be the rooted quadrangulation obtained by adding an edge e going, with the infinite face on its right, from the origin s of d to the point t diametrically opposed to s in the outer face of d. As d has no inner decomposition path, the argument used in the first part of the proof ensures that q has no separating 4-cycle. Hence q is irreducible and, by construction, q has image d by the injection of Section 8.2. □

Lemma 26 and Theorem 25 ensure that $\mathcal{U}_{n-4}$ is in bijection with $\mathcal{P}'_n$ and that $\mathcal{U}'_{ij}$ is in bijection with $\mathcal{P}'_{ij}$. Hence the enumeration of rooted 3-connected maps according to the number of edges and according to the number of vertices and faces comes down to the enumeration of $\mathcal{U}'_n$ and of $\mathcal{U}'_{ij}$.

The decomposition.

Lemma 27 *Let d be a rooted irreducible dissection. Let $\mathcal{P}_1$ and $\mathcal{P}_2$ be two decomposition paths of d. Then three cases can arise for the intersection $\mathcal{P}_1 \cap \mathcal{P}_2$:*

- *$\mathcal{P}_1 \cap \mathcal{P}_2 = \{s, t\}$. In this case $\mathcal{P}_1$ and $\mathcal{P}_2$ are said internally disjoint.*
- *There exists an inner vertex v connected to s by an edge e such that $\mathcal{P}_1 \cap \mathcal{P}_2 = \{s\} \cup \{t\} \cup \{v\} \cup \{e\}$. In this case $\mathcal{P}_1$ and $\mathcal{P}_2$ are said upper joint.*
- *There exists an inner vertex v connected to t by an edge e such that $\mathcal{P}_1 \cap \mathcal{P}_2 = \{s\} \cup \{t\} \cup \{v\} \cup \{e\}$. In this case $\mathcal{P}_1$ and $\mathcal{P}_2$ are said down joint.*

Proof. It is easy to check that all other configurations for $\mathcal{P}_1 \cap \mathcal{P}_2$ are excluded using the two following arguments:

- The dissection d has no multiple edge (which is an easy consequence of the fact that d has no separating 4-cycle).
- There can not exist a cycle of edges of d having an odd number of edges (which is an easy consequence of the fact that the degrees of the faces of d are even).

□

Lemma 27 implies in particular that two decomposition paths can not cross each other. Hence the decomposition paths of an irreducible dissection d can be ordered from left to right. We denote by $\{\mathcal{P}_0, \ldots, \mathcal{P}_l\}$ the series of decomposition paths of d ordered from left to right, so that $\mathcal{P}_0$ is the left border path of d and $\mathcal{P}_l$ is the right border path of d.

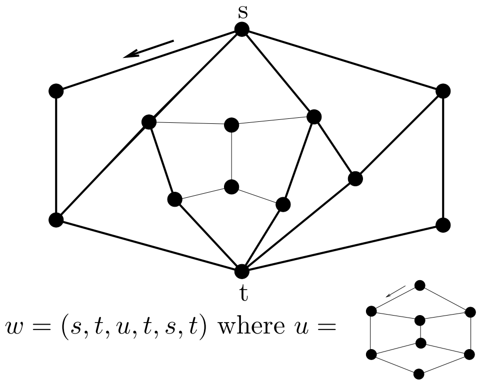

Figure 14: Example of the decomposition of a rooted irreducible dissection and of its associated decomposition word.

Lemma 28 *Let d be a rooted irreducible dissection and let $\mathcal{P}_1$ and $\mathcal{P}_2$ be two decomposition paths of d that are upper joint (resp. down joint). Then the interior of the area delimited by $\mathcal{P}_1$ and $\mathcal{P}_2$ consists of a unique face incident to s (resp. to t).*

Proof. This is a trivial consequence of the fact that the interior of each 4-cycle of d is a face. □

Decomposition word of a dissection. Let $d \in \mathcal{D}'$ and let $\{\mathcal{P}_0, \ldots, \mathcal{P}_l\}$ be the series of decomposition paths of d ordered form left to right. Then we define the alphabet $\mathcal{A} = \{s\} \cup \{t\} \cup \mathcal{U}'$, consisting of two letters s and t and of letters which are each identified with an object of $\mathcal{U}'$. We can associate to d a word of length l an $\mathcal{A}$ in the following way, see Figure 14.

For each $0 \leq i \leq l-1$, three cases can arise:

- $\mathcal{P}_i$ and $\mathcal{P}_{i+1}$ are internally disjoint. Then the map delimited by $\mathcal{P}_i$ and $\mathcal{P}_{i+1}$, and rooted at the first edge of $\mathcal{P}_i$ with the vertex s as origin, is a rooted undecomposable dissection u. Then we put the letter u at place i of w.
- $\mathcal{P}_i$ and $\mathcal{P}_{i+1}$ are upper joint. Then we place the letter s at place i of w.
- $\mathcal{P}_i$ and $\mathcal{P}_{i+1}$ are down joint. Then we place the letter s at place i of w.

The fact that this coding is injective is an easy consequence of Lemma 28.

Caracterisation of the words corresponding to the coding of an element of $\mathcal{D}'$. The fact that d has no separating 4-cycle implies easily that its associated word can not have two successive s nor two successive t. It is also easy to see that this is the the only condition letting d have a separating 4-cycle.

In addition, the fact that d is a dissection of the hexagon implies that the word associated to d is not the empty word nor the one-letter words s or t. It is easy to see that all other words code dissections of the hexagon.

Hence the set $\mathcal{D}'$ is in bijection with non empty words on $\mathcal{A}$ different from s and t and not containing the factor ss or tt.

Equations linking the generating functions of $\mathcal{D}'$ and of $\mathcal{U}'$. The preceding caracterisation of the words corresponding to the coding of elements of $\mathcal{D}'$ allows to obtain the following two equations.

Let $D(x)$ (resp. $U(x)$ be the generating function of $\mathcal{D}'$ (resp. of $\mathcal{U}'$) counted according to the number of inner faces. Then we have the equation:

$$D(x) = \left(\frac{2x}{1-x} + 1\right) \frac{1}{1 - U(x)\left(\frac{2x}{1-x} + 1\right)} - 2x - 1$$

This allows to obtain the coefficients of $U(x)$ from the coefficients of $D(x)$, which are known from Corollary 10.

Similarly, let $D(x_\bullet, x_\circ) = \sum |\mathcal{D}'_{ij}| x_\bullet^{i+2} x_\circ^{j+2}$ and let $U(x_\bullet, x_\circ) = \sum |\mathcal{U}'_{ij}| x_\bullet^{i+2} x_\circ^{j+2}$.

Then the caracterisation of the coding words gives:

$$\begin{aligned} D(x_\bullet, x_\circ) &= (1 + x_\bullet) \frac{1}{1 - x_\circ x_\bullet} (1 + x_\circ) \\ &\quad \cdot \frac{1}{1 - U(x_\bullet, x_\circ)(1 + x_\bullet)\frac{1}{1 - x_\circ x_\bullet}(1 + x_\circ)} \\ &\quad - x_\bullet - x_\circ - 1 \end{aligned}$$

9 Sampling rooted 3-connected planar maps

9.1 Sampling rooted 3-connected maps with n edges.

We deduce from the first application of Theorem 9 the following algorithm:

- Sample an object a of $\mathcal{B}'_{n-4}$.

- Perform the closure of a to obtain an irreducible dissection $d \in \mathcal{D}_{n-4}$. Choose randomly one of the 6 edges of the hexagon of d to carry the root.
- Add an edge e in the outer face of d going, with the infinite face on its right, from the origin v of the root of d to the vertex diametrically opposed to v in the outer face of d. Carry the root on e with v as origin of the root[7]. The obtained figure is a rooted quadrangulation q with n faces.
- If q is irreducible, return the rooted 3-connected map in $\mathcal{P}'_n$ associated to q by Tutte's application. Otherwise reject.

Proposition 29 *We have the asymptotic result:*

$$\frac{|\mathcal{P}'_n|}{|\mathcal{D}'_{n-4}|} \sim \frac{2^8}{3^6}$$

Hence the distribution for the number of rejects is a geometric law whose mean is $c = \frac{3^6}{2^8}$. Hence, as the closure application has a linear-time complexity, the sampling algorithm has a linear-time complexity.

Proof. We have obtained in section 6 the enumerative result $|\mathcal{D}'_n| = \frac{6}{n+2}|\mathcal{B}'_n| = \frac{6(2n)!}{(n+2)!n!}$. Using Stirling formula, we obtain $|\mathcal{D}'_{n-4}| \sim \frac{3}{128\sqrt{\pi}}\frac{4^n}{n^{5/2}}$. Moreover, according to [31], $|\mathcal{P}'_n| \sim \frac{2}{3^5\sqrt{\pi}}\frac{4^n}{n^{5/2}}$. □

9.2 Sampling rooted 3-connected maps with i vertices and j faces.

Using the second application of Theorem 9, we have the following algorithm to sample rooted 3-connected maps with i vertices and j faces:

- Sample an object a of $\mathcal{B}'_{i-3,j-3}$. We describe a simple linear-time algorithm in section A.2 to perform the random generation of objects of $\mathcal{B}'_{ij}$.
- Perform the closure of a to obtain an irreducible dissection d with i black vertices and j white vertices. Choose randomly the root among the three edges of the hexagon whose origin v is a black vertex.
- Add an edge e in the outer face of d going with the infinite face on its right from the origin v of the root of d to the vertex diametrically opposed to v in the outer face of d. Carry the root on e with v as origin of the root. The obtained figure is a rooted quadrangulation q with i black vertices and j white vertices.
- If q is irreducible, return the rooted 3-connected map in $\mathcal{P}'_{ij}$ associated to q by Tutte's application. Otherwise reject.

Proposition 30 *If we fix a ratio $\alpha \in]1/2, 2[$ for the quantity $\frac{i}{j}$, then we have the asymptotic result:*

$$\frac{|\mathcal{P}'_{ij}|}{|\mathcal{D}'_{ij}|} \sim \frac{2^8}{3^6}\frac{(2-\alpha)^2(2\alpha-1)^2}{\alpha^2}$$

Hence the distribution for the number of rejects is a geometric law whose mean is $c_\alpha = \frac{3^6}{2^8}\frac{\alpha^2}{(2-\alpha)^2(2\alpha-1)^2}$. Hence, when the ratio α is fixed, the sampling algorithm has a linear-time complexity with a constant factor proportional to c_α.

Moreover, in the worst case of triangulations where $j = 2i - 4$, the mean number of rejects is quadratic, hence the sampling algorithm is quartic.

Proof. These asymptotic results are easy consequences of the enumerative result $|\mathcal{D}'_{ij}| = \frac{3}{2i-j+1}|\mathcal{B}'_{ij}| = \frac{3}{(2i+1)(2j+1)}\binom{2j+1}{i}\binom{2i+1}{j}$ obtained in Section 6 and of the asymptotic result $|\mathcal{P}'_{ij}| \sim \frac{1}{3^5 2^4 ij}\binom{2i-2}{i+2}\binom{2j-2}{j+2}$ given in [3]. □

10 Random planar graphs

The algorithm of [4] to generate labelled planar graphs is based on the decomposition of graphs into a tree-like structure of 3-connected components. In other terms there is a decomposition of any planar graph p into a pair $(t, (a_1, \ldots, a_k))$, where each a_k is a rooted 3-connected planar graph (*i.e.* the shape of the kth component) and t is the tree-like structure (*i.e.* the necessary information to glue components and put labels). A fundamental property of the uniform distribution on planar graphs is that given t (and in particular the numbers of vertices i_k and edges n_k in each connected components), the a_k are independant and uniformly distributed on $\mathcal{P}(n_k, i_k, j_k)$.

[7]This operation is the inverse of the injection of section 8.2.

The algorithm then essentially consists into generating the tree-like structure with the right probability, and then generating random 3-connected components with an external generator as [28]. The generation of the tree-like structure can be done by the recursive method [23] because all branching probabilities can be explicitely computed. The approach used in [4] consists in precomputing all the $O(n^4)$ entries involved in the branching probabilities by direct dynamical programming, *i.e.* applying convolutive recurrences, for a total cost of $O(n^6)$ arithmetic multiplications on numbers with $O(n \log n)$ bits.

Once the precomputation is done, the cost of generating the tree-like shape is small in front of the cost of generating the 3-connected graphs. In [4], the generation is done using the random sampler proposed in [28], and the cost of this part of the generation was estimated to $O(n^{13/2})$. However this analysis fails for extremal ranges of values, due to uniformity assumptions stated in the complexity results of [28], and ignored in [4]. For instance generating connected planar graphs with $2n$ edges and $i = n$ vertices amounts to generating triangulations, which are 3-connected. In this case the whole process boils down to one call of the generator of [28], that has exponential complexity.

The new generator that we have proposed here allows both to correct this problem and to improve the complexity. Indeed in view of Proposition 30, the sampler has at most quartic complexity, and it is called to generate a linear number of edges. The final complexity of the generation is thus $O(n^3)$.

11 Optimal encoding of 3-connected planar maps

11.1 Introduction

We recall that a planar map without multiple edge is said *3-connected* if at least 3 vertices must be removed to disconnect the map.

We describe a simple algorithm to encode a 3-connected planar map whose outer face is triangular. Hence it can also be used to encode a general 3-connected planar map G. Indeed, if the outer face of G is not triangular, it suffices to fix three consecutive vertices a_1, a_2 and a_3 on the outer face of G and link a_2 and a_3 by an edge to obtain a 3-connected planar map $\widetilde{G}$ whose outer face is triangular. Then the coding of G is obtained as the coding of $\widetilde{G}$ and a bit indicating that we had to add an edge.

The idea of the algorithm of coding is very close from the algorithm of opening of an irreducible dissection and uses the concepts that we have introduced in Section 7 to prove that the application of opening is correctly defined. In particular, we use the concepts of derivated map and of α_0-orientation of a derivated map. An example of the execution of the algorithm is illustrated on Figure 15.

11.2 Description of the algorithm of coding

Compute the minimal α_0-orientation of the derivated map. Let G be a 3-connected planar map whose outer face is triangular. Doing a traversal of the outer face of G with the outer face on our left, we denote by a_1, a_2 and a_3 the vertices of the outer face. We denote by G' the derivated map of G. To compute the minimal α_0-orientation of G', we have found an iterative linear-time algorithm which is very similar to the algorithm of Kant of right-most canonical ordering. We describe this algorithm in Section 12.

Associate a dissection d of the hexagon with quadrangular faces to the derivated map. We can associate to the derivated map G' a bicolored dissection d of the hexagon with quadrangular faces by inversing the construction of Section 7.3. Thus the vertices of d are the primal and dual vertices of G'. The edges of d are obtained as follows: each inner face f of G' is quadrangular, has two edge-vertices and has a primal and a dual vertex which are diagonally opposed. The edge of d associated to f is obtained by linking the primal vertex and the dual vertex of f by a new edge, see Figure 15c where the derivated map is superposed with its associated dissection of the hexagon (ignore the orientations until next paragraph). Using 3-connectivity of G and reasoning similarly as in the proof of Lemma 19, it is easy to prove that d is irreducible. More precisely, d is a bicolored complete irreducible dissection. Hence G' is the derivated map of d in the sense of Section 7.3.

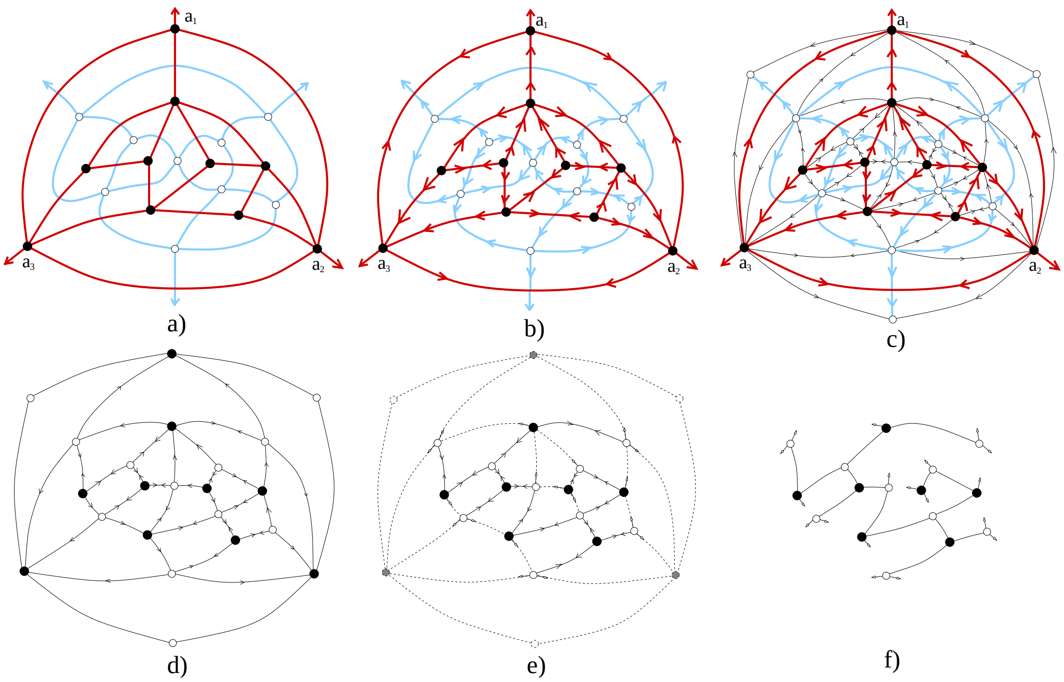

Figure 15: The execution of the encoding algorithm on an example.

Compute the complete-tri-orientation of d without clockwise cycle from the minimal α_0-orientation of G'. As explained in Section 7.6, by applying the inverse of the transposition rules for orientations, we get the complete-tri-orientation without clockwise cycle of d from the α_0-orientation of G' without clockwise cycle.

Open the dissection d in a binary tree a. We apply here the algorithm of opening of d endowed with its complete-tri-orientation without clockwise cycle, noted $\tilde{t}$. Thus we compute first the tri-orientation t without clockwise cycle of d from $\tilde{t}$. As explained in section 7.2, this comes down to compute the image of $\tilde{t}$ by the application Ψ. Then we perform the opening of d by removing the edges and vertices of the hexagon of d and by disconnecting all simply oriented edges of d at their extremity.

Encode the binary tree a. First we choose an arbitrary bud of a and root a at this bud. Then we have to encode the obtained rooted binary tree.

If we encode 3-connected planar maps with n edges, we always obtain a binary tree with $n' = n-5$ inner vertices, see Section 9.1. It is a classical result that the set of rooted binary trees with n' inner vertices can be optimally encoded with Dyck-words of length $2n'$.

If we encode 3-connected planar maps with i vertices and j faces, we always obtain a rooted binary tree such that its canonical bicoloration has $i' = i-3$ black vertices and $j' = j-3$ white vertices. The set of rooted binary trees whose canonical bicoloration has i' black vertices and j' white vertices can also be optimally encoded, see section A.1.

12 Description of the algorithm computing the minimal α_0-orientation of the derivated map

12.1 Idea of the algorithm

Let G be a 3-connected planar graph whose outer face is triangular and let G' be its derivated map. We denote by a_1, a_2 and a_3 the border vertices of G. We describe here a linear-time iterative algorithm to compute the minimal α_0-orientation of G'. The idea is to maintain at each step k a simple cycle $\mathcal{C}_k$ of edges of G such that:

- The edge (a_2, a_3) is on $\mathcal{C}_k$.
- For each edge e of G outside of $\mathcal{C}_k$, the 4 edges of G' incident to the edge-vertex v_e associated

to e have been oriented at a step $j < k$ and v_e has outdegree 1.

- All other edges of G' are not oriented yet.

In the following, we note G_k the submap of G obtained by removing all vertices and edges outside of $\mathcal{C}_k$. In addition, we order the vertices of the cycle $\mathcal{C}_k$ from left to right, i.e. by doing a traversal of $\mathcal{C}_k$ from a_3 to a_2 without passing by the edge (a_2, a_3).

12.2 Labelling the half-edges of G

During the algorithm, when we orient an edge e' of G' corresponding to an half-edge of G, we also give a label 1, 2 or 3 to e'. Indeed we don't need these labels to perform the algorithm of orientation, but they will be very useful to prove that the algorithm really computes the minimal α_0-orientation. These labels also correspond to the Schnyder Woods of G', introduced in [13].

For the labels, we also have to maintain a few invariants during the algorithm:

- At each step k, each vertex v of G outside of $\mathcal{C}_k$ has one outgoing edge in each label 1, 2 and 3 and these outgoing edges are in clockwise order around v. In addition, all edges between the outgoing edges with labels i and $i+1$ are incoming with label $i-1$, see Figure 16a.

- Let v be a vertex on $\mathcal{C}_k$ having at least one incident edge of G' outside of G_k. Then exactly one of these edges, noted e'_1, is going out of v. In addition it has label 1. The edges of $G\backslash G_k$ incident to v and between e'_1 and its left neighbour on $\mathcal{C}_k$ are incoming and labelled 2. Similarly, the edges incident to v in $G\backslash G_k$ between e'_1 and its right neighbour are incoming and labelled 3, see Figure 16b.

- For each edge e of G outside of G_k, let e' be the unique outgoing edge of v_e. Two cases can occur:

  - If e' is an half-edge of G then the two edges of G' incident to v_e and forming the edge e are identically labelled.

  - If e' is an half-edge of G^*, we note $1 \leq i \leq 3$ the label of the edge of G' succeeding e' in the clockwise order around v_e. Then the edge of G' succeeding e' in the counter-clockwise order around v_e is labelled $i+1$, see Figure 16c.

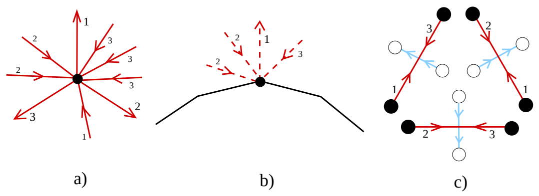

Figure 16: The invariants concerning the labels of the half-edges of G and maintained during the algorithm.

12.3 Description of step k of the algorithm

Introduction Let us now describe the k^{th} step of the algorithm. During this step, we remove vertices of $\mathcal{C}_k$ and we remove their incident edges. Thus their incident bounded faces are merged with the infinite face of G_k. For each removed edge e, we also orient the 4 incident edges in G' of its associated edge-vertex v_e and we label the two incident edges of v_e corresponding to the two half-edges of e.

In this way, we obtain a new planar graph, noted G_{k+1}, and we have to choose the vertices removed from $\mathcal{C}_k$ in such a way that the contour $\mathcal{C}_{k+1}$ of G_{k+1} is still a simple cycle containing (a_2, a_3).

Definitions A vertex of $\mathcal{C}_k$ is said *active* if it is incident to at least one edge of $G\backslash G_k$. Otherwise, the vertex is said *passive*. By convention, before the first step of the algorithm, the vertex a_1 is considered as active and its incident half-edge directed toward the infinite face is labelled 1.

For each couple of vertices (v_1, v_2) of $\mathcal{C}_k$ ordered such that v_1 is on the left of v_2 on the contour of $\mathcal{C}_k$, the border path on $\mathcal{C}_k$ to go from v_1 to v_2 without passing by the edge (a_2, a_3) is denoted by $[v_1, v_2]$. We also use the notation $]v_1, v_2[= [v_1, v_2]\backslash\{v_1, v_2\}$.

A couple $\{v_1, v_2\}$ of vertices is said *separating* if there exists an inner face f of G_k such that v_1 and v_2 are incident to f but the edges of $[v_1, v_2]$ are not all incident to f. Such a face is called a *separating face* and the triple (v_1, v_2, f) is called a *separator*. The area delimited by the border path $[v_1, v_2]$ and by the path of edges of f going from v_1 to v_2

with the interior of f on its right is called the *separated area* of (v_1, v_2, f) and noted $Sep(v_1, v_2, f)$. We also define the *interior of the separated area* of (v_1, v_2, f) as $Sep(v_1, v_2, f)\backslash[v_1, v_2]$.

The inclusion-relation on the separated areas induces a partial order on the separators.

A vertex v on $\mathcal{C}_k$ is said *blocked* if it is incident to a separating face of G_k. In particular, v does not belong to any separating couple of vertices. An important remark is that the vertices a_2 and a_3 are always blocked. Indeed the edge (a_3, a_2), which has the infinite face of G on its right, is not equal to the path $[a_3, a_2]$, otherwise the simple cycle $\mathcal{C}_k$ would be reduced to the edge (a_2, a_3).

A vertex v on $\mathcal{C}_k$ is said *eligible* if it is active and not blocked.

Finally, for each vertex v of $\mathcal{C}_k$, we define its *left-connection vertex* v_{left} as the leftmost vertex on $\mathcal{C}_k$ such that the vertices of $]v_{left}, v[$ all have only two incident edges in G_k. The path $[v_{left}, v]$ is called the *left-chain* of v and the first edge of $[v_{left}, v]$ is called the *left-connection edge* of v. Similarly, we define the *right-connection vertex*, the *right-chain*, and the *right-connection edge* of v.

An important remark is that all vertices of $]v_{left}, v[$ and of $]v, v_{right}[$ are active. Indeed these vertices have two incident edges in G_k but they have at least 3 incident edges in G because G is 3-connected. Hence they have at least one incident edge in $G\backslash G_k$.

Operations of step k First we choose the rightmost eligible vertex of $\mathcal{C}_k$ and we call $v^{(k)}$ this vertex [8]. Remark that this eligible vertex can not be a_2 or a_3 because a_2 and a_3 are blocked.

We note $f_1, \ldots, f_m$ the bounded faces of G_k incident to $v^{(k)}$ from right to left. We also note $e_1, \ldots, e_{m+1}$ the edges of G_k incident to $v^{(k)}$ from right to left. Hence, $\forall 1 \leq i \leq m$, f_i corresponds to the sector between e_i and e_{i+1}.

An important remark is that the right-chain of $v^{(k)}$ is reduced to one edge. Indeed if there exists a vertex in $]v^{(k)}, v^{(k)}_{right}[$, then v is active as already explained, and v is incident to a unique inner face of G_k, which is f_1. As f_1 is incident to $v^{(k)}$ and as $v^{(k)}$ is non blocked, f_1 is not separating. Hence v is not blocked. Thus v is eligible and is on the right

[8] We will prove in Lemma 32 that there always exists an eligible vertex on $\mathcal{C}_k$ as long as G_k is not reduced to the edge (a_2, a_3).

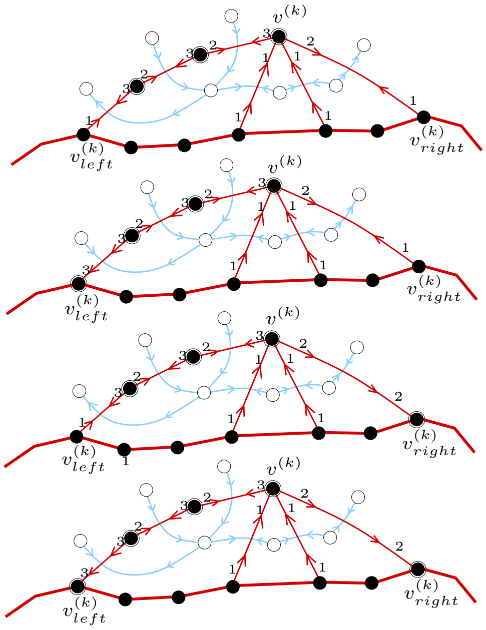

Figure 17: The operations performed at step k of the algorithm, whether $v^{(k)}_{left}$ and $v^{(k)}_{right}$ are active or not.

of $v^{(k)}$, in contradiction with the fact that $v^{(k)}$ is the rightmost eligible vertex on $\mathcal{C}_k$.

We perform the following operations on the edges of G' incident to the edge-vertices of the left-chain of $v^{(k)}$ and of the edges $e_1, \ldots e_m$, see Figure 17, where the active vertices are surrounded:

- For each edge e_i with $2 \leq i \leq m$, we note v_{e_i} the corresponding edge-vertex of G'. We orient the two edges of G' forming e_i toward $v^{(k)}$ and give label 1 to these two edges. We orient the two other incident edges of v_{e_i} toward v_{e_i}, so that v_{e_i} has outdegree 1.
- Traversing the left-chain of v^k from $v^{(k)}$ to $v^{(k)}_{left}$, let e be an edge of the chain different from the left-connection edge of $v^{(k)}$. Then we bi-orient e and label 3 (resp. label 2) the first traversed (resp. the second traversed) half-edge of e. The unique outgoing edge of the edge-vertex v_e associated to e is chosen to be the edge going out of e on the left of e.
- If $v^{(k)}_{left}$ is passive, we bi-orient the left-connection edge e of $v^{(k)}$. Traversing e toward $v^{(k)}_{left}$, we label 3 the first traversed half-edge and label 1 the second traversed half-edge of e. We choose

the unique outgoing edge of the edge-vertex v_e to be the edge going out of v_e on the right of e. If $v^{(k)}_{left}$ is active, we label 3 and orient toward $v^{(k)}_{left}$ the two edges of G' forming e and we orient the two other incident edges of v_e toward v_e.

- We treat the edge e_1, which is the right-connection edge of $v^{(k)}$, similarly as the left-connection edge. If $v^{(k)}_{right}$ is passive, we bi-orient e_1. Going from $v^{(k)}$ to $v^{(k)}_{right}$, we label 2 the first traversed half-edge of e_1 and label 1 the second traversed half-edge of e_1. We choose the unique outgoing edge of v_{e_1} as the edge going out of v_{e_1} on the left of e_1. If $v^{(k)}_{right}$ is active, we orient the two half-edges of e_1 toward $v^{(k)}_{right}$ and label them 2. We orient the two other incident edges of v_{e_1} toward v_{e_1}.

Finally the graph G_{k+1} is obtained from G_k by removing the edges of the left-chain of $v^{(k)}$, the edges $e_1, \dots, e_m$, the vertex $v^{(k)}$ and the vertices of $]v^{(k)}_{left}, v^{(k)}[$.

As a_2 and a_3 are blocked on $\mathcal{C}_k$, the contour of G_{k+1} still contains the edge (a_3, a_2).

In addition, if G_{k+1} is not reduced to (a_2, a_3), the 3-connectivity of G and the fact that the chosen vertex $v^{(k)}$ is not incident to any separating face can be used to prove easily that the contour $\mathcal{C}_{k+1}$ of G_{k+1} is a simple closed curve, i.e. it does not contain any separating vertex.

In addition, we see on Figure 17 that the operations performed at step k maintain the invariants of labelling and maintain the fact that all edge-vertices outside of G_{k+1} have their 4 incident edges oriented and have outdegree 1.

In view of proving that the algorithm terminates, we state the following lemma:

Lemma 31 *Let (v_1, v_2, f) be a separator on $\mathcal{C}_k$. Then there exists an eligible vertex in $]v_1, v_2[$.*

Proof. Let (v'_1, v'_2, f') be a minimal separator for the (non empty) set of separators whose separated area is included or equal to the separated area of (v_1, v_2, f). Hence v'_1 and v'_2 are in $[v_1, v_2]$.

Suppose that no vertex of $]v'_1, v'_2[$ is active. The path $[v'_1, v'_2]$ and the path to go from v'_1 to v'_2 with the interior of f' on its right can not be both reduced to an edge, because there can not be any multiple edges in a 3-connected planar map. Hence one of these two paths contains a vertex v different from v_1 and v_2. As we suppose that no vertex of $]v_1, v_2[$ is connected to $G \backslash G_k$, the removal of v_1 and v_2 would disconnect v from the other part of $G \backslash \{v_1, v_2\}$, which is non empty. This is in contradiction with the fact that G is 3-connected.

Hence there exists an active vertex v in $]v'_1, v'_2[$, which is also in $]v_1, v_2[$. If v was incident to a separating face, this face would be included in the area separated by (v'_1, v'_2, f'), which is impossible by minimality of (v'_1, v'_2, f'). Hence the active vertex v is also not blocked, thus v is eligible. $\Box$

We state the following lemma, which ensures that the algorithm terminates:

Lemma 32 *There exists an eligible vertex on $\mathcal{C}_k$.*

Proof.

Suppose that there exists no separating couple of vertices on $\mathcal{C}_k$. In this case, we just have to prove that there exists an active vertex on $\mathcal{C}_k$. At the first step of the algorithm, there exists an active vertex on $\mathcal{C}_1$ because a_1 is said active by convention. At any other step, there exists trivially an active vertex on $\mathcal{C}_k$, otherwise G_k would be disconnected from $G \backslash G_k$, which is non empty.

If there exists at least one separator (v_1, v_2, f), Lemma 31 ensures that there exists an eligible vertex v in $]v_1, v_2[$. $\Box$

Finishment of the algorithm. Lemma 32 implies that there remains just the edge $e = (a_2, a_3)$ at the end of the algorithm. To finish the algorithm, we bi-orient (a_2, a_3) and label 3 (resp. label 2) the half-edge of e whose origin is a_2 (resp. a_3). In addition, for the edge-vertex v_e associated to e, its outgoing edge is chosen to be its incident edge directed toward the infinite face. We also label respectively 2 and 3 the half-edges incident to a_2 and a_3 and directed toward the infinite face.

Figure 18 illustrates the execution of the algorithm on an example. On this figure, the edges of $\mathcal{C}_k$ are black and wider. In addition, the active vertices are surrounded and the next chosen vertex is doubly surrounded. This algorithm is similar to the algorithm of [18], which can be implemented with a linear-time complexity. The adaptation of these methods of implementation ensures that our algorithm has also a linear-time complexity.

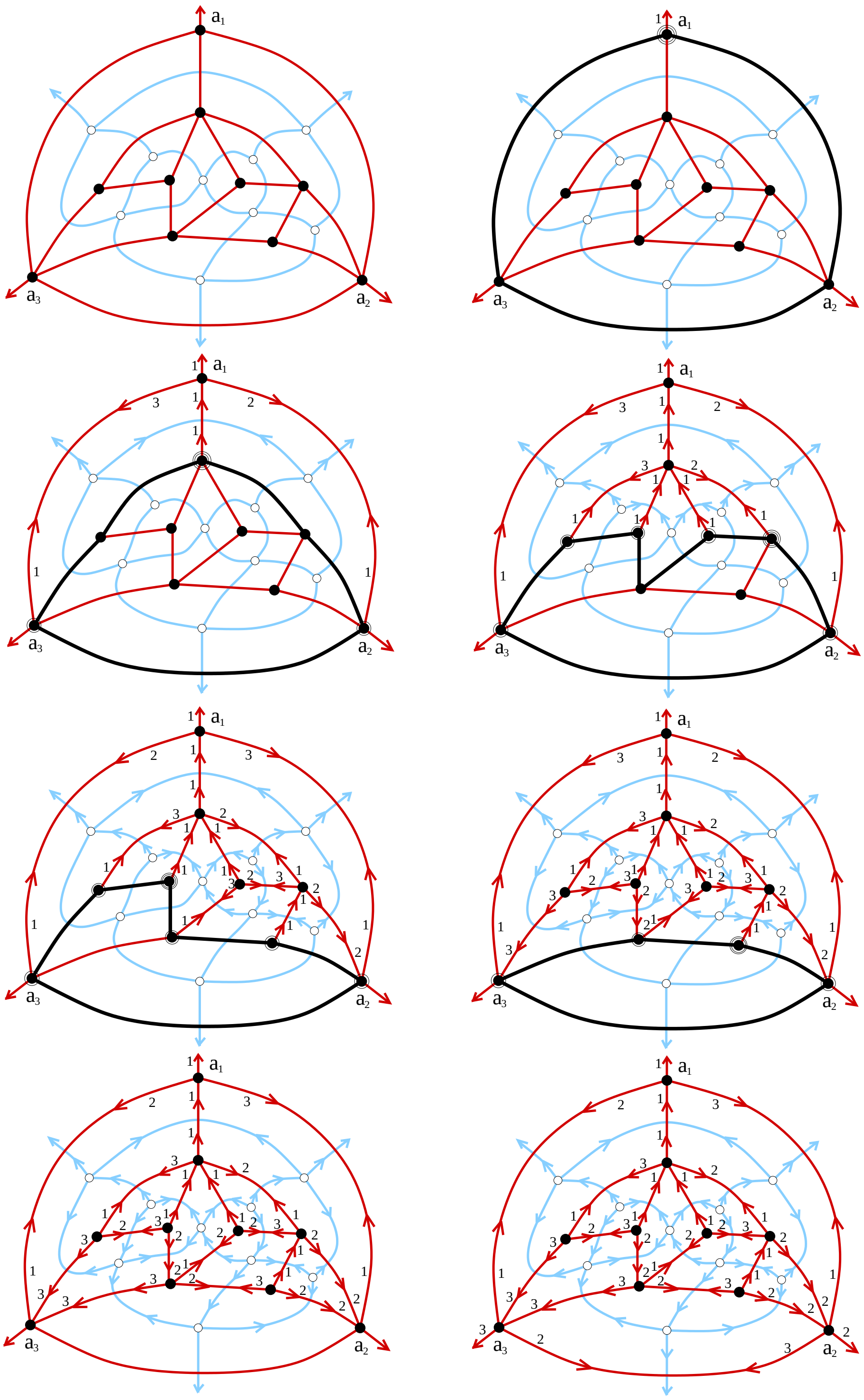

Figure 18: The execution of the algorithm of orientation on an example.

Theorem 33 *The algorithm computes the minimal α_0-orientation of the derivated map.*

The proof of this theorem is the object of the next section 33.

Our algorithm computes the minimal α_0-orientation and the associated Schnyder Woods of the derivated map of a 3-connected planar graph. In fact, our algorithm generalizes an algorithm computing the Schnyder Woods of a triangulation and presented in [7].

13 Proof of Theorem 33

In all this section, we denote by X_0 the α_0-orientation computed by the algorithm.

13.1 The algorithm computes an α_0-orientation

By construction of the algorithm, each primal vertex of the derivated map G' has one outgoing edge for each label 1, 2 and 3, hence it has outdegree 3. By construction also, each edge-vertex of G' has outdegree 1. Hence it just remains to prove that each dual vertex of G' has outdegree 3 in X_0.

Let f be an inner face of G and let v_f be its corresponding dual vertex in G^*. Let k be the step during which f has been merged with the infinite face of G. During this step, a series of consecutive edges of f have been removed. We call *upper path* this path of removed consecutive edges. We call *lower path* of f the series of edges of f that are not in the upper path of f. By construction of the algorithm (see Figure 17), exactly two edges of G' connecting v_f to an edge-vertex of the upper path of f are going out of v_f.

Hence it just remains to prove that exactly one edge of G' connecting v_f to an edge-vertex of the lower path of f is going out of v_f. First remark that the lower path P of f is a non empty path of edges on the border $\mathcal{C}_{k+1}$ of G_{k+1} and that the two extremities v_l and v_r of this path are active on $\mathcal{C}_{k+1}$, see Figure 17. In addition, all vertices of $]v_l, v_r[$ are passive on $\mathcal{C}_{k+1}$. The fact that exactly one edge of G' connecting v_f to an edge-vertex of P is going out of v_f is a direct consequence of the following lemma, see Figure 19.

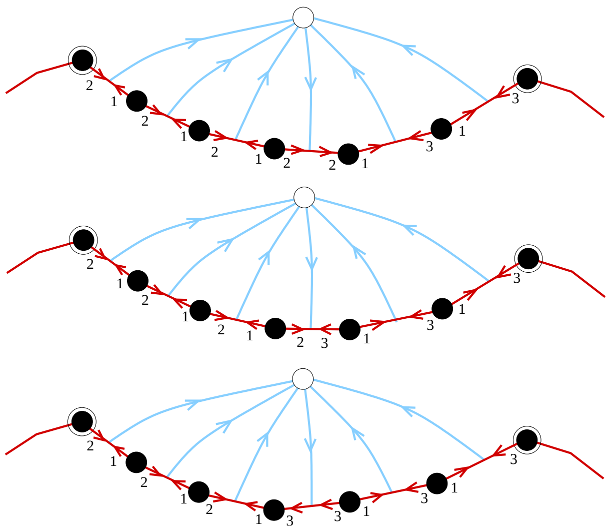

Figure 19: The dual vertex of a face f has one outgoing edge connected to the lower path of f.

Lemma 34 *At a step k of the algorithm, let v_1 and v_2 be two active vertices on $\mathcal{C}_k$ such that all vertices of $]v_1, v_2[$ are passive. Then the path $[v_1, v_2]$ on $\mathcal{C}_k$ is divided in three consecutive areas:*

- *A (possibly empty) path $[v_1, v]$ whose edges are bi-oriented, leaving the left-vertex of each edge with label 2 and entering the right-vertex of each edge with label 1.*
- *An edge $e = [v, v']$ that is either simply oriented with label 2 from v to v' or simply oriented with label 3 from v' to v or bi-oriented, leaving v with label 2 and entering v' with label 3.*
- *A (possibly empty) path $[v', v_2]$ of bi-oriented edges leaving the left-vertex of each edge with label 1 and entering the right-vertex of each edge with label 3*

Proof. The proof is by recurrence on the length of $[v_1, v_2]$. Suppose that this length is equal to 1. Then $[v_1, v_2]$ is reduced to an edge. If v_1 is removed at an earlier step than v_2, then the edge (v_1, v_2) is simply oriented with label 2 from v_1 to v_2. If v_2 is removed at an earlier step than v_1, then the edge (v_1, v_2) is simply oriented with label 3 from v_2 to v_1. If v_1 and v_2 are removed at the same step, then (v_1, v_2) is bi-oriented, leaving v_1 with label 2 and entering v_2 with label 3, see Figure 17.

Suppose now that the length of $[v_1, v_2]$ is at least 2. Remark first that the outer path $[v_1, v_2]$ remains unchanged as long as none of v_1 or v_2 is removed. This remark follows from the fact that all vertices of $]v_1, v_2[$ are passive, hence no vertex of $[v_1, v_2]$ can be treated as long as none of v_1 or v_2 is treated.

Then two cases can arise: if v_1 is removed before v_2, then the right neighbour v of v_1 becomes active and the edge (v_1, v) is bi-oriented leaving v_1 with label 2 and entering v with label 1. Similarly if v_2 is removed before v_1, then the left neighour v of v_2 becomes active and the edge (v, v_2) is bi-oriented leaving v_2 with label 3 and entering v with label 1.

The result follows by recurrence, with a recursive call of the path $[v, v_2]$ in the first case and of the path $[v_1, v]$ in the second case. □

Remark that we do not need the fact that we choose at each step the rightmost eligible vertex. Hence the algorithm can be easily adapted to compute an α_0-orientation of G' whatever the choice of an eligible vertex at each step is.

13.2 The algorithm computes the minimal α_0-orientation of the derivated map

Definition of maximal bi-labelled paths. Let v be a vertex of G. For $1 \leq i \leq 3$ we define the i-path of v and denote by P_v^i the unique oriented path $(v_0, \ldots, v_m)$ starting at v and such that each edge (v_p, v_{p+1}) is the outgoing edge of v_p with label i. For $1 \leq i \leq 3$ and $1 \leq j \leq 3$ with $i \neq j$, we define the maximal $i-j$ path starting at v as follows. Let $l \leq m$ be the maximal index such that the subpath $(v_0, \ldots, v_l)$ of P_v^i only consists of bi-oriented edges leaving their origin with label i and entering their extremity with label j. Then the maximal $i-j$ path starting at v is defined to be the path $(v_0, \ldots, v_l)$ and is denoted by P_v^{i-j}.

Premilinary lemmas. At a step $k \geq 2$, let $v^{(k)}$ be the chosen vertex, i.e. the rightmost eligible vertex on $\mathcal{C}_k$.

We claim that there exists an active vertex on the right of $v^{(k)}$. Indeed, the rightmost vertex a_2 is active as soon as $k \geq 2$ and a_2 is non eligible on $\mathcal{C}_k$ because it is blocked, hence a_2 is different from $v^{(k)}$. Hence a_2 is an active vertex on the right of $v^{(k)}$

We define the next active vertex on the right of $v^{(k)}$ as the unique vertex v on the right of $v^{(k)}$ on $\mathcal{C}_k$ such that all vertices of $]v^{(k)}, v[$ are passive.

Lemma 35 *At a step $k \geq 2$, let $v^{(k)}$ be the chosen vertex. Let v be the next active vertex on the right of $v^{(k)}$. Let v_{prec} be the left neighbour of v on $\mathcal{C}_k$. Then each edge of $[v^{(k)}, v_{prec}]$ is bi-oriented, leaving with label 2 its left vertex and entering with label 1 its right vertex. The edge $e = (v_{prec}, v)$ is either simply oriented with label 2 from v_{prec} to v or bi-oriented, leaving v_{prec} with label 2 and entering v with label 3. Otherly speaking, $P_{v^{(k)}}^{2-1} = [v^{(k)}, v_{prec}]$ and the outgoing edge of v_{prec} with label 2 is (v_{prec}, v).*

Proof. To prove this lemma, using the result of Lemma 35, we just have to prove that (v_{prec}, v) is neither bi-oriented leaving v_{prec} with label 1 and entering v with label 3, nor simply oriented with label 3 from v to v_{prec}, see Figure 19.

First remark that the active vertex v is on the right of $v^{(k)}$, hence it can not be eligible, hence v is blocked.

As a consequence there exists a vertex v' and a face f such that v, v' and f form a separator. Lemma 31 ensures that there exists an eligible vertex in $]v', v[$, hence the vertex v' is on the left of $v^{(k)}$ on $\mathcal{C}_k$, otherwise $v^{(k)}$ would not be the rightmost eligible vertex. Let P be the path of f going from v to v' with the interior of f on its left. Two cases can arise: if the first edge of P is different from (v, v_{prec}), then v_{prec} is above P. Hence v_{prec} is in the interior of the separated area of (v', v, f), hence v_{prec} will be treated (removed) at an earlier step than v. As v is active, it implies (see Figure 17) that (v_{prec}, v) is simply oriented with label 2 from v_{prec} to v.

Suppose now that the first edge of P is (v, v_{prec}). Remark that v_{prec} can not be equal to v'. Indeed v is on the right of $v^{(k)}$, hence v_{prec} is on the right or equal to $v^{(k)}$, whereas v' is on the left of $v^{(k)}$.

Hence P has a length greater than 1. As a consequence, when f will cease to be separable, v_{prec} will only be incident to f. Figure 17 ensures that, when such a vertex v_0 is removed, the edge connecting v_0 to its right neighbour is always bi-oriented and bi-labelled 2-3 from v_0 to its right neighbour, which concludes the proof of the lemma. □

Lemma 36 *At a step $k \geq 2$, let $v^{(k)}$ be the chosen vertex. Let v be the next active vertex on the right of $v^{(k)}$. Let v^{3-2} be the extremity of P_v^{3-2} and let e be the outgoing edge of v^{3-2} with label 3. If e*

is bi-oriented [9], *define* $v_1 = v^{3-2}$. *If* e *is simply oriented, define* v_1 *as the extremity of* e.

Then v_1 *belongs to* $\mathcal{C}_k$ *and is on the left of* $v^{(k)}$.

Proof. First remark that each vertex v'' such that the couple $\{v'', v\}$ is separating is on the left of $v^{(k)}$. Otherwise, Lemma 31 ensures that there exists an eligible vertex in $]v, v''[$. As v is on the right of $v^{(k)}$, this is in contradiction with the fact that $v^{(k)}$ is the rightmost eligible vertex.

Remark also that the set of separators (v'', v, f) involving v and endowed with the inclusion-relation is not only a partial order but a total order. In particular for two separators (v''_1, v, f) and (v''_2, v, f), if v''_1 is on the left of v''_2, then the separated area of (v''_2, v, f) is included in the separated area of (v''_1, v, f). In addition, this set is non empty because v is the next active vertex on the right of $v^{(k)}$, hence v is blocked.

Let (v', v, f) be the maximal separator for this totally ordered set. Then the separated area of (v', v, f) contains all separating faces incident to v except f. Let P be the path of edges of f going from v to v' with the interior of f on its left. We denote by B the interior of the separated area of (v', v, f). Let $\widetilde{G_k}$ be the submap of G obtained by removing B from G_k. Let $\widetilde{\mathcal{C}_k}$ be the contour of $\widetilde{G_k}$.

We claim that f is not separating in $\widetilde{G_k}$. Otherwise, there would exist a vertex v_2 on the right of v such that (v, v_2, f) is a separator or there would exist a vertex v_3 on the left of v' such that (v_3, v, f) is a separator: the first case is in contradiction with the fact that all separators $\{v, v_2\}$ involving v are such that v is on the right of v_2. The second case is in contradiction with the fact that (v', v, f) is the maximal separator involving v.

We claim that only vertices of B will be removed from step k on, until all vertices of B are removed. Indeed, all separating faces incident to vertices on the right of v are faces of $\widetilde{G_k}$, hence they will remain separating as long as not all vertices of B are removed. As all vertices on the right of v are either blocked or passive, it is easy to show inductively that all these vertices will keep the same status until all vertices of B are removed.

Let k_0 be the first step where all vertices of B have been removed. Then $G_{k_0} = \widetilde{G_k}$, hence f is not separating anymore on $\mathcal{C}_{k_0}$ but all other separating faces of $\widetilde{G_k}$ are still separating in $\widetilde{G_k}$. Moreover, all separating faces incident to v at step k were the face f and faces in B. In addition, all faces of $\widetilde{G_k}$, except f, have kept their separating-status between step k and step k_0. Hence v is eligible on $\mathcal{C}_{k_0}$.

In addition, the rightmost eligible vertex $v^{(k_0)}$ at step k_0 is a vertex incident to f. It is either v or a vertex $\tilde{v}$ of f on the right of v on $\mathcal{C}_{k_0}$ and such that $[v, \tilde{v}]$ only consists of edges incident to f (otherwise f would be separating).

Moreover, the left-connection vertex of $v^{(k_0)}$ is v'. Otherwise there would be a vertex of f on $\widetilde{\mathcal{C}_k}$ and on the left of v'. In addition, this vertex would also be on $\mathcal{C}_k$ because only the vertices of B are removed to obtain $\widetilde{G_k}$ from G_k. This is in contradiction with the fact that (v', v, f) is the maximal separator of $\mathcal{C}_k$ involving v.

Then two cases can arise: either v' is passive or v' is active on $\mathcal{C}_{k_0}$.

Suppose that v' is passive on $\mathcal{C}_{k_0}$. Then v' is not incident to any edge of $G \backslash \widetilde{G_k}$. In particular v' is not incident to any edge of B. Hence the right neighbour of v' on $\mathcal{C}_{k_0}$ and on $\mathcal{C}_k$ are the same vertex, which is also the vertex preceding v' on P. We denote this vertex by v_1. Remark that v_1 is on the left of $v^{(k)}$ on $\mathcal{C}_k$ (indeed, v_1 can not be equal to $v^{(k)}$ at step k because v_1 is incident to f, which is separating at this step). Then, by construction of the algorithm (see Figure 17), $P^{3-2}_{v^{(k_0)}}$ is the border path on $\mathcal{C}_{k_0}$ going from $v^{(k_0)}$ to v_1 and (v_1, v') is bi-oriented bi-labelled $3-1$ from v_1 to v'. As $v \in [v_1, v^{(k_0)}] \backslash \{v_1\}$ on $\mathcal{C}_{k_0}$, P^{3-2}_v is also the border path on $\mathcal{C}_{k_0}$ going from v to v_1 and (v_1, v') is bi-oriented bi-labelled $3-1$ from v_1 to v'.

Suppose that v' is active on $\mathcal{C}_{k_0}$. We denote the vertex v' by v_1. Remark that the vertex v_1 is a vertex on $\mathcal{C}_k$ on the left of $v^{(k)}$. By construction of the algorithm (see Figure 17) and using a similar argument as in the last paragraph, P^{3-2}_v is the border path on $\mathcal{C}_{k_0}$ to go from v to the right neighbour of v_1 on $\mathcal{C}_{k_0}$ and the edge connecting the right neighbour of v_1 to v_1 is simply oriented with label 3 toward v_1. □

Lemma 37 *The vertices* a_1, a_2 *and* a_3 *can not belong to any clockwise cycle.*

Proof. We reason here with a_1 (the cases of a_2

[9] Note that in this case, e is bi-labelled 3-1 from v^{3-2} to v_1 by definition of a maximal bi-labelled path.

and a_3 can be treated identically). The outgoing edge of a_1 with label 1 is directed toward the infinite face. The outgoing edges of a_1 with labels 2 and 3 connect respectively a_1 to two edge-vertices whose unique outgoing edge is directed toward the infinite face. Hence each directed path starting at a_1 finishes directly in the infinite face. $\square$

The contour of any face of G' is not a clockwise cycle. In view of proving that the α_0-orientation X_0 computed by the algorithm has no clockwise cycle, the first step is to prove the following lemma:

Lemma 38 *Let f be an inner face of G'. Then the contour of f is not a clockwise cycle in X_0.*

Proof. Suppose that the contour of f is a clockwise cycle. We recall that the contour of f has two edge-vertices, one dual vertex, and one primal vertex v. Let i be the label of the edge e' of f going out of v. The edge e' is the first half-edge of an edge e of G. We denote by v_e the edge-vertex of G' associated to e and by v' the vertex of G such that $e = (v, v')$. As the contour of f is a clockwise cycle, the unique outgoing edge of v_e succeeds the edge (v_e, v) in the counter-clockwise order around v_e. Hence, according to Figure 16c, the edge e is bi-oriented and the second half-edge of e has label $i+1$. We denote by e_{next} the edge of G succeeding e in the clockwise order around v. The edge e'_{next} of G' succeeding e' in the clockwise order around v is the edge of f directed toward v. Hence the rules of labelling ensure that e'_{next} has label $i-1$. As e'_{next} is the second half-edge of e_{next}, this ensures that e_{next} is simply oriented with label $i-1$ toward v.

Suppose that $i = 1$, so that the edge e is bi-labelled 1-2 from v to v' and e_{next} is simply oriented with label 3 toward v. Let k be the step of the algorithm during which the vertex v' is removed from G_k. Figure 17 ensures that, if v' is not equal to the rightmost eligible vertex $v^{(k)}$, then the outgoing edge with label 2 of v' is bi-oriented and its other label is 3, which is not the case here. Hence $v' = v^{(k)}$, see Figure 20.

In addition, as (v', v) is bi-labelled 2-1 from v' to v, the vertex v is passive on $\mathcal{C}_k$. Hence, noting $e_{v\to}^{(k)}$ the edge of $\mathcal{C}_k$ whose left extremity is v, there can not be any edge of $G\backslash G_k$ between e and $e_{v\to}^{(k)}$ in the clockwise order around v. Hence $e_{v\to}^{(k)} = e_{next}$.

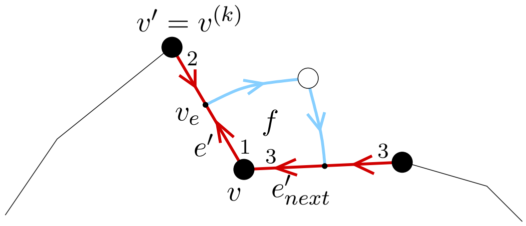

Figure 20: The configuration yielded by the presence of a face f of G' whose contour is a clockwise cycle and such that the outgoing edge of the unique primal vertex of f has label 1.

We claim that $k \geq 2$. Otherwise v' would be equal to a_1. As $e = (v', v)$ is bi-labelled 1-2 from v to v', v would be equal to a_2. But according to Lemma 37, a_2 can not belong to any clockwise cycle.

Hence $k \geq 2$ and we can use Lemma 35. In particular, this lemma ensures that $e_{v\to}^{(k)}$ is the outgoing edge of v with label 2. We obtain here a contradiction with the fact that e_{next} is going toward v with label 3 and that $e_{v\to}^{(k)} = e_{next}$.

Suppose now that $i = 2$, so that e is bi-labelled 2-3 from v to v' and e_{next} is simply oriented with label 1 toward v. Let k be the step during which v is removed from G_k. By construction of the algorithm (see Figure 17), the vertex v belongs to $]v_{left}^{(k)}, v^{(k)}[$ and e_{next} is the outgoing edge of v with label 3. This is in contradiction with the fact that e_{next} is simply oriented toward v with label 1.

Finally suppose that $i = 3$, so that e is bi-labelled 3-1 from v to v' and e_{next} is simply oriented with label 2 toward v. Let $\underline{v}$ be the origin of e_{next} and let k be the step during which $\underline{v}$ is removed from G_k. As e_{next} is simply oriented with label 2 from $\underline{v}$ to v, we have $\underline{v} = v^{(k)}$ and $v = v_{right}^{(k)}$ (see Figure 17). Hence $v_{right}^{(k)}$ is the next active vertex on the right of $v_{right}^{(k)}$ on $\mathcal{C}_k$. In addition $k \geq 2$, otherwise $v^{(k)} = a_1$, in contradiction with the fact that the outgoing edge of a_1 with label 2 is bi-oriented. Hence, we can use Lemma 36: in our case, the next active vertex on the right of $v^{(k)}$ is v and the path P_v^{3-2} is empty because the outgoing edge with label 3 of v is bi-labelled 3-1. Hence the vertex denoted by v_1 in the statement of Lemma 36 is here v. Then Lemma 36 ensures that v is a vertex of $\mathcal{C}_k$ on the left of $v^{(k)}$, in contradiction with the fact that v is the right neighbour of $v^{(k)}$ on $\mathcal{C}_k$. $\square$

Possible configurations for the contour of a minimal clockwise cycle of X_0.

Lemma 39 *A minimal clockwise cycle in an α_0-orientation X of G' is turnright-most.*

Proof. Let $\mathcal{C}$ be a minimal clockwise cycle of X, i.e. a clockwise cycle whose interior is not included in the interior of any other clockwise cycle. Suppose that $\mathcal{C}$ is not turnright-most. Hence there exists a vertex v_0 on $\mathcal{C}$ which is either a primal or a dual vertex and such that an outgoing edge e' of v_0 is in the interior of $\mathcal{C}$. Let $\mathcal{P}_{e'}$ be the turnright-most path starting at e'.

We claim that $\mathcal{P}_{e'}$ can not pass twice by the same vertex in the interior of $\mathcal{C}$. Indeed, let v be the first vertex by which $\mathcal{P}_{e'}$ passes twice. When $\mathcal{P}_{e'}$ returns to v, it encloses a simple oriented close curve $\mathcal{C}'$ whose interior is included in $\mathcal{C}$. But $\mathcal{C}'$ can not be counter-clockwise according to Lemma 23 and $\mathcal{C}'$ can not be clockwise by minimality of $\mathcal{C}$. Hence $\mathcal{P}_{e'}$ can not pass twice by the same vertex in the interior of $\mathcal{C}$.

Thus $\mathcal{P}_{e'}$ has to reach $\mathcal{C}$ at a vertex v_1. Let $\widetilde{\mathcal{P}_{e'}}$ be the part of $\mathcal{P}_{e'}$ between v_0 and v_1 and let $c_1 \subset \mathcal{C}$ be the oriented path going from v_1 to v_0. Then the concatenation of $\widetilde{\mathcal{P}_{e'}}$ and c_1 is a clockwise cycle whose interior is included in the interior of $\mathcal{C}$, which is impossible by minimality of $\mathcal{C}$. $\square$

Lemma 40 *Let $\mathcal{C}$ be a minimal clockwise cycle of X_0. Let m be the submap of G' obtained by removing all vertices and edges that are in the exterior of $\mathcal{C}$. Then all edge-vertices on $\mathcal{C}$ have more than 2 incident edges in m.*

Proof. Let v_e be an edge-vertex of $\mathcal{C}$ having only two incident edges in m, i.e. the incident edges of v_e in m are the two edges of $\mathcal{C}$ incident to v_e. Let v_1 (resp. v_2) be the primal or dual vertex preceding (resp. succeeding) v_e on $\mathcal{C}$. Let e' be the edge of G' succeeding (v_1, v_e) in the clockwise order around v_1. Lemma 39 ensures that the minimal clockwise cycle $\mathcal{C}$ is turnright-most, hence e' is directed toward v_1. Let f be the face of G' on the right of the angle formed by e' and (v_1, v_e), so that e', (v_1, v_e) and (v_e, v_2) are three consecutive edges of f. The orientation of e', (v_1, v_e) and (v_e, v_2) and the fact

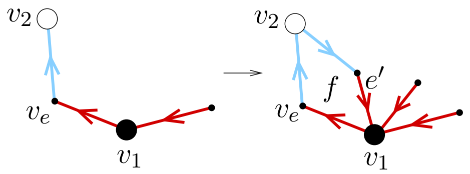

Figure 21: The existence of an edge-vertex v_e on a minimal clockwise cycle $\mathcal{C}$, such that v_e has no incident edge in the interior of $\mathcal{C}$, yields the presence of a face f whose contour is a clockwise cycle.

that all edge-vertices of X_0 have outdegree 1 ensure that the contour of f is a clockwise cycle, see Figure 21. This is in contradiction with Lemma 38. $\square$

Lemma 41 *Let $\mathcal{C}$ be a minimal clockwise cycle of X_0 and let m be the submap of G' obtained by removing all edges and vertices of G' that are outside of $\mathcal{C}$. Define $n_e^{(2)}$, $n_e^{(3)}$ and $n_e^{(4)}$ to be the number of edge-vertices on $\mathcal{C}$ which have respectively 2, 3 and 4 incident edges in m. Lemma 40 ensures that $n_e^{(2)} = 0$. In addition, $2n_e^{(3)} + n_e^{(4)} = 6$.*

Proof. We use the notations of Lemma 23. Thus, we denote by n_v and n_f the respective numbers of primal and dual vertices of m. We denote by $n_e^{(int)}$ the number of inner edge-vertices of m, and we denote by e and f the respective numbers of edges and faces of m. Finally we denote respectively by b and k the quantities $2n_e^{(2)} + 3n_e^{(3)} + 4n_e^{(4)}$ and $n_e^{(2)} + n_e^{(3)} + n_e^{(4)}$. According to Lemma 40, $n_e^{(2)} = 0$ for the orientation X_0. Hence, $b = 3n_e^{(3)} + 4n_e^{(4)}$ and $k = n_e^{(3)} + n_e^{(4)}$.

Euler relation on m is $(n_v + n_f + n_e^{(int)} + k) + f = e + 1$. All inner faces have degree 4 and there are $2k$ edges on the border of m, hence $4f = 2e - 2k$. In addition, counting the edges of m according to the degree of all edge-vertices of m gives $e = 4n_e^{(int)} + b$. Using these two last equalities, Euler relation becomes $n_v + n_f + \frac{1}{2}k = n_e^{(int)} + \frac{1}{2}b + 1$.

The edges of m can also be counted according to their origin in X_0. As $\mathcal{C}$ is turnright-most, the k primal or dual vertices on the border of m only have one outgoing edge in m. All inner primal or dual vertices of m have outdegree 3 in m and all edge-vertices of m have outdegree 1 in m. Hence the counting of the edges of m according to their origin gives $e = (3n_v + 3n_f - 2k) + (n_e^{(int)} + k)$.

Injecting Euler relation in this equality, we obtain $e = 4n_e^{(int)} + \frac{3}{2}b + 3 - \frac{5}{2}k$. Combining this equality with $e = 4n_e^{(int)} + b$, we obtain $\frac{5}{2}k = \frac{1}{2}b + 3$. Hence $5k = b + 6$, hence $5n_e^{(3)} + 5n_e(4) = 3n_e(3) + 4n_e(4) + 6$. Finally we have $2n_e^{(3)} + n_e(4) = 6$. $\square$

Using Lemma 41, we can list all possible configurations for a minimal clockwise cycle of X_0. These configurations are represented on Figure 22, up to a rotation.

Each configuration of Figure 22 is impossible for a clockwise cycle of X_0. In the last section, we have restricted the number of possible configurations for a clockwise cycle of X_0. In this section, we present the method which ensures that the presence of a clockwise cycle for each configuration of Figure 22 yields a contradiction.

The method is based on the use of Lemma 35, of Lemma 36, and of the following lemma:

Lemma 42 *At a step k, let v and v' be two vertices on $\mathcal{C}_k$ such that v is on the left of v'. Suppose that there exists a path $P = (v_0, \ldots, v_l)$ of edges of G such that $v_0 = v$, $v_l = v'$, and for each $0 \leq i \leq l-1$, the edge (v_i, v_{i+1}) is the outgoing edge of v_i with label 1. Then $P = [v, v']$ and all edges of P are bi-oriented.*

Proof. To prove that $P = [v, v']$, it suffices to prove that all edges of P are on $\mathcal{C}_k$.

By construction of the algorithm (see Figure 17), for each vertex v_0 of G, the extremity v_1 of the outgoing edge of v_0 with label 1 is treated (removed) at an earlier step than v_0. Hence, as each vertex v_0 of $G \backslash G_k$ has been removed at a step $j < k$, the extremity v_1 of the outgoing edge of v_0 with label 1 is also in $G \backslash G_k$. Hence, if P passes by a vertex outside of G_k, it can not reach $\mathcal{C}_k$ again. By definition of an active vertex of $\mathcal{C}_k$, the extremity of its outgoing edge with label 1 is a vertex of $G \backslash G_k$. Hence none of the vertices $v_0, \ldots v_{l-1}$ can be active, otherwise P would pass by a vertex outside of G_k and could not reach $\mathcal{C}_k$ again, in contradiction with the fact that P ends at a vertex of $\mathcal{C}_k$.

Hence all vertices by which P passes before reaching v' are passive. It just remains to prove that the outgoing edge with label 1 of each passive vertex of $\mathcal{C}_k$ is a bi-oriented edge of $\mathcal{C}_k$.

Let v_0 be a passive vertex of $\mathcal{C}_k$ and let $v_{0,l}$ and $v_{0,r}$ be respectively the left and the right neighbour of v_0 on $\mathcal{C}_k$. We claim that the outgoing edge of v_0 with label 1 is the edge $(v_0, v_{0,l})$ if $v_{0,l}$ will be removed before $v_{0,r}$ and is the edge $(v_0, v_{0,r})$ if $v_{0,r}$ will be removed before $v_{0,l}$. Indeed, as long as none of $v_{0,l}$ or $v_{0,r}$ is removed, v_0 remains passive and keeps $v_{0,l}$ and $v_{0,r}$ as left and right neighbour. Let k_0 be the first step where $v_{0,l}$ or $v_{0,r}$ is removed. First, by construction of the algorithm, two vertices v_1 and v_2 on the contour of $\mathcal{C}_{k_0}$ such that $]v_1, v_2[$ contains a passive vertex can not be removed at the same step. Hence, at step k_0, either $v_{0,l}$ or $v_{0,r}$ is removed. Suppose that the removed vertex at step k_0 is $v_{0,l}$. Then, at step k_0, $(v_0, v_{0,l})$ is given a bi-orientation and is bi-labelled 1-2 from v_0 to $v_{0,l}$, see Figure 17. Similarly, if the removed vertex is $v_{0,r}$ then, at step k_0, $(v_0, v_{0,r})$ is given a bi-orientation and is bi-labelled 1-3 from v_0 to $v_{0,r}$. $\square$

We take here the example of the 3^{th} configuration of the case $\{n_e^{(3)} = 2, n_e^{(4)} = 2\}$ of Figure 22. Let $\mathcal{C}$ be a clockwise cycle corresponding to such a configuration. Then there are on $\mathcal{C}$ two successive dual edges e_1^* and e_2^* in the counter-clockwise order around $\mathcal{C}$ and a unique primal vertex that we denote by $v_{\mathcal{C}}$.

Let m' be the submap of G' obtained by removing all edges and vertices outside of $\mathcal{C}$. Let m be the submap of G obtained by keeping only the edges whose associated edge-vertex belongs to m' and by keeping the vertices incident to these edges.

The rules of labelling (see Figure 16), the fact that all edge-vertices have outdegree 1, and the fact that $\mathcal{C}$ is turnright-most determine unambiguously the labels and orientations of all the edges of the contour of m, up to the label of the outgoing edge of $v_{\mathcal{C}}$ on $\mathcal{C}$. Figures 23a, 23b and 23c represent the respective configurations when the label of the outgoing edge of $v_{\mathcal{C}}$ on $\mathcal{C}$ is 1, 2 or 3.

First we treat the case of Figure 23a. Let $\hat{v}$ (resp. $\widehat{v_0}$) be the primal vertex outside of $\mathcal{C}$ and incident to the edge-vertex associated to e_2^* (resp. e_1^*). Let $\widehat{v'}$ be the primal vertex inside of $\mathcal{C}$ and incident to the edge-vertex associated to e_2^*. Let k be the step at which $\hat{v}$ is removed from G.

As already explained in preceding proofs (for example in the proof of Lemma 38), it is easy to

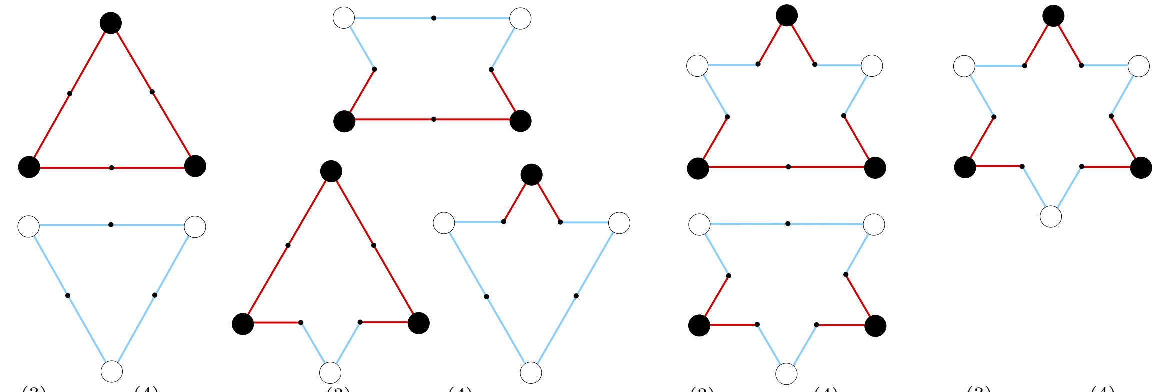

Figure 22: The possible configurations for a minimal clockwise cycle of X_0.

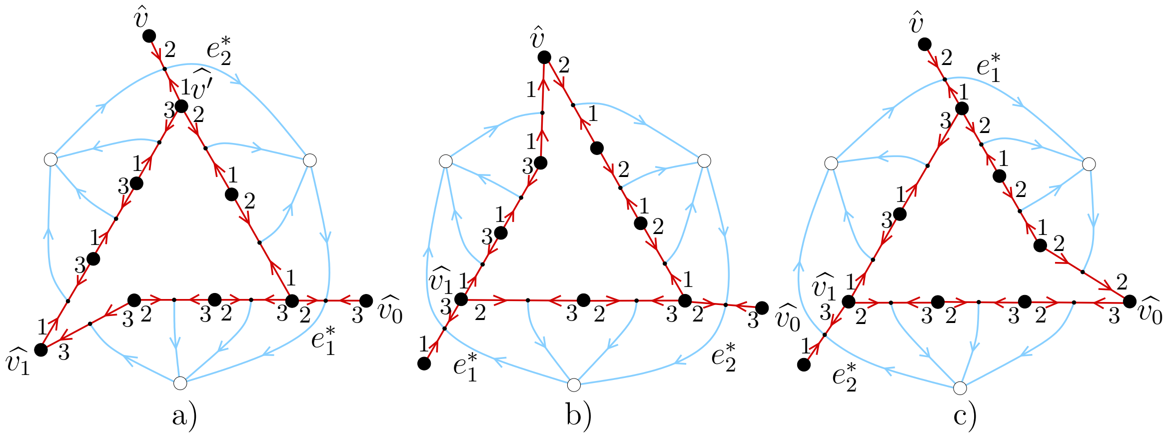

Figure 23: The 3 possible cases for the contour of the map m associated to the 3^{th} configuration of the case $\{n_e^{(3)} = 2, n_e^{(4)} = 2\}$ of Figure 22.

see that $k \geq 2$ and that $\hat{v}$ is the chosen vertex $v^{(k)}$. Hence we can use Lemma 35 and Lemma 36. In addition $\widehat{v'}$ is the right neighbour of $\hat{v}$ on $\mathcal{C}_k$.

Lemma 35 and the configuration of Figure 23a ensure that $\widehat{v_0}$ is the next active vertex on the right of $\hat{v}$ on $\mathcal{C}_k$. Moreover, the configuration of Figure 23a ensures that $\widehat{v_1}$ corresponds to the vertex v_1 of the statement of Lemma 36. Hence Lemma 36 ensures that $\widehat{v_1}$ is on $\mathcal{C}_k$ on the left of $\hat{v}$. We see on Figure 23a that there is an oriented path P going from $\widehat{v_1}$ to $\widehat{v'}$ such that each edge of the path is leaving with label 1. Lemma 42 ensures that $P = [\widehat{v_1}, \widehat{v'}]$, in contradiction with the fact that, on Figure 23a, the edge of $\mathcal{C}_k$ connecting $\widehat{v'}$ to its left neighbour $\hat{v}$ is leaving $\hat{v}$ with label 2.

We treat the case of Figure 23b similarly. We note $\hat{v} = v_{\mathcal{C}}$. We note $\widehat{v_0}$ the primal vertex outside of $\mathcal{C}$ and incident to the edge-vertex associated to e_2^*. We note $\widehat{v_1}$ the primal vertex inside of $\mathcal{C}$ and incident to the edge-vertex associated to e_1^*.

Let k be the step where $\hat{v}$ is removed. Then it is easy to see that $k \geq 2$ and $\hat{v} = v^{(k)}$. Hence we can use Lemma 35 and Lemma 36.

Lemma 35 and the configuration of Figure 23b ensure that $\widehat{v_0}$ is the next active vertex on the right of $\hat{v}$ on $\mathcal{C}_k$. Then we see on Figure 23b that the vertex $\widehat{v_1}$ corresponds to the vertex v_1 of the statement of Lemma 36. Hence Lemma 36 ensures that $\widehat{v_1}$ is on $\mathcal{C}_k$ on the left of $\hat{v}$. We see on Figure 23b that there exists an oriented path P going from $\widehat{v_1}$ to $\hat{v}$ such that each edge of P leaves with label 1. But we see on Figure 23b that the last edge of P is simply oriented, in contradiction with Lemma 42.

Finally the case of Figure 23c can be treated similarly (we have placed the vertices $\widehat{v_0}$, $\widehat{v_1}$ and $\hat{v}$).

A similar treatment ensures that each other configuration of Figure 22 can not be the contour of a clockwise cycle of X_0. This concludes the proof of Theorem 33.

Acknowledgements. N. Bonichon and L. Castelli Aleardi are thanked for fruitful discussions.

References

[1] P. Alliez and C. Gotsman. Recent advances in compression of 3d meshes. In *Proceedings of the Symposium on Multiresolution in Geometric Modeling*, Cambridge, 2003. available on `http://www.cs.technion.ac.il/~gotsman/`.

[2] J. Ambjørn, P Białas, Z. Burda, J. Jurkiewicz, and B. Petersson. Effective sampling of random surfaces by baby universe surgery. *Phys. Lett. B*, 325:337–346, 1994.

[3] E. A. Bender. The number of three-dimensional convex polyhedra. *Amer. Math. Monthly*, 94(1):7–21, 1987.

[4] M. Bodirsky, C. Gröpl, and M. Kang. Generating labeled planar graphs uniformly at random. In *ICALP*, pages 1095–1107, 2003.

[5] N. Bonichon, C. Gavoille, and N. Hanusse. An information-theoretic upper bound of planar graphs using triangulation. In *STACS*, pages 499–510, 2003.

[6] J. Bouttier, P. di Francesco, and E. Guitter. Census of planar maps: from the one-matrix solution to a combinatorial proof. *Nucl. Phys. B*, 645:477–499, 2002.

[7] E. Brehm. 3-orientations and schnyder 3-tree-decompositions. `http://page.mi.fu-berlin.de/~felsner/Diplomarbeiten/brehm.ps.gz`.

[8] L. Castelli-Aleardi and O. Devillers. Canonical triangulation of a graph, with a coding application. preprint, 2004.

[9] R. C.-N. Chuang, A. Garg, X. He, M.-Y. Kao, and H.-I Lu. Compact encodings of planar graphs via canonical orderings. In *ICALP*, pages 118–129, 1998.

[10] H. de Frayssex, P. Ossona de Mendez, and P. Rosenstiehl. *Pigale, Automatic Graph Drawing.* Atelier de taxiplanie, CAMS, EHESS, Paris. ALCOM-IT, ESPRIT LTR Projet 20244.

[11] A. Denise, M. Vasconcellos, and D. J. A. Welsh. The random planar graph. *Congr. Numer.*, 113:61–79, 1996. Festschrift for C. St. J. A. Nash-Williams.

[12] S. Felsner. Convex drawings of planar graphs and the order dimension of 3-polytopes. *Order*, 18:19–37, 2001.

[13] S. Felsner. Lattice structures for planar graphs. *Electron. J. Comb.*, 11(1):Research paper R15, 24p, 2004.

[14] P. Flajolet, P. Zimmermann, and B. Van Cutsem. A calculus for random generation of labelled combinatorial structures. *Theoret. Comput. Sci.*, 132(2):1–35, 1994.

[15] C. Gotsman. On the optimality of valence-based connectivity coding. *Computer Graphics Forum*, pages 99–102, 2003.

[16] X. He, M.-Y. Kao, and H.-I Lu. Linear-time succinct encodings of planar graphs via canonical orderings. *SIAM J. on Discrete Mathematics*, 12(3):317–325, 1999.

[17] X. He, M.-Y. Kao, and H.-I Lu. A fast general methodology for information-theoretically optimal encodings of graphs. *SIAM J. Comput*, 30(3):838–846, 2000.

[18] G. Kant. Drawing planar graphs using the canonical ordering. *Algorithmica*, 16:4–32, 1996. (also *FOCS'92*).

[19] A. Khodakovsky, P. Alliez, M. Desbrun, and P. Schröder. Near-optimal connectivity encoding of 2-manifold polygon meshes. *Graphical Model*, 64(3–4), 2002.

[20] H.-I Lu. Linear-time compression of bounded-genus graphs into information-theoretically optimal number of bits. In *SODA*, pages 223–224, 2002.

[21] C. McDiarmid, A. Steger, and D. Welsh. Random planar graphs. 20pp, 2003.

[22] J. Ian Munro and Venkatesh Raman. Succinct representation of balanced parentheses, static trees and planar graphs. In 38^{th} *Annual IEEE Symposium on Foundations of Computer Science (FOCS)*, pages 118–126. IEEE Computer Society Press, October 1997.

[23] A. Nijenhuis and H. S. Wilf. *Combinatorial Algorithms*. Academic Press, second edition, 1978.

[24] D. Osthus, H. J. Prömel, and A. Taraz. On random planar graphs, the number of planar graphs and their triangulations. *J. Combin. Theory Ser. B*, 88(1):119–134, 2003.

[25] D. Poulalhon and G. Schaeffer. Optimal coding and sampling of triangulations. In *ICALP*, pages 1080–1094, 2003.

[26] J. Rossignac. Edgebreaker: Connectivity compression for triangle meshes. *IEEE Transactions on Visualization and Computer Graphics*, 5(1):47–61, 1999.

[27] G. Schaeffer. Bijective census and random generation of Eulerian planar maps with prescribed vertex degrees. *Electron. J. Combin.*, 4(1):Research Paper 20, 14 pp., 1997.

[28] G. Schaeffer. Random sampling of large planar maps and convex polyhedra. In *STOC*, pages 760–769, 1999.

[29] W. Schnyder. Embedding planar graphs on the grid. In *SODA*, pages 138–148, 1990.

[30] C. Touma and C. Gotsman. Triangle mesh compression. In *Graphic Interface Conference*, pages 26–34, 1998.

[31] W. T. Tutte. A census of planar maps. *Canad. J. Math.*, 15:249–271, 1963.

[32] D. B. Wilson. An annotated bibliography of perfectly random sampling with markov chains. Maintained on `http://dimacs.rutgers.edu/~dbwilson/exact`.

[33] D. B. Wilson. Determinant algorithms for random planar structures. In *SODA*, pages 258–267, 1997.

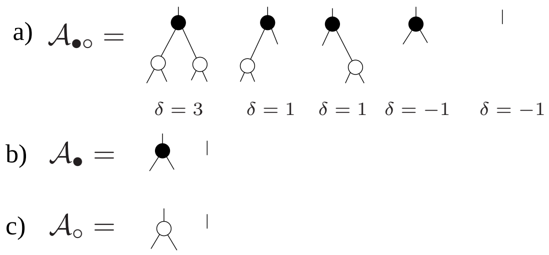

Figure 24: The three alphabets used respectively for the words $w_{\bullet\circ}$, $w_{\bullet}$ and $w_{\circ}$ associated to a bicolored binary tree.

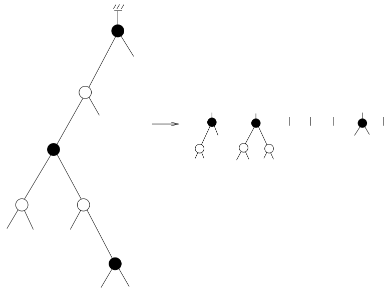

Figure 25: A bicolored planted binary tree and its associated word on $\mathcal{A}_{\bullet\circ}$.

A Encoding and sampling bicolored planted binary trees

A.1 Encoding

We explain here how to encode the objects of $\mathcal{B}'_{ij}$. Let $a \in \mathcal{B}'_{ij}$. Doing a depth-first traversal of a from left to right, we obtain a word $w_{\bullet\circ}$ of length $(2j+1)$ on the alphabet $\mathcal{A}_{\bullet\circ}$, (this alphabet is represented on Figure 24a), see Figure 25 for an example. It is easy to see that the sum of the weights of the letters of any strict prefix of $w_{\bullet\circ}$ is nonnegative and the sum of the weights of the letters of $w_{\bullet\circ}$ is equal to -1. In addition, $w_{\bullet\circ}$ is the unique word in its cyclic equivalence-class which has these two properties.

Then we can transform $w_{\bullet\circ}$ into a couple $(w_{\bullet}, w_{\circ})$ of words such that:

- $w_{\bullet}$ is a word of length $(2j+1)$ on the alphabet $\mathcal{A}_{\bullet}$ (this alphabet is represented on Figure 24b) with i black-vertex-letters.
- $w_{\circ}$ is a word of length $2i$ on the alphabet $\mathcal{A}_{\circ}$ (this alphabet is represented on Figure 24c) with j white-vertex-letters.

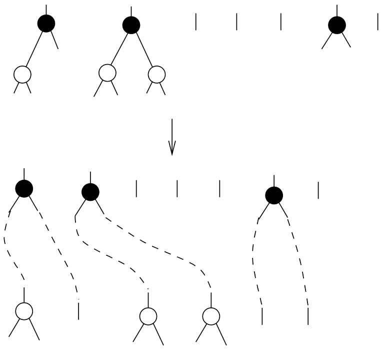

Figure 26: The word $w_{\bullet\circ}$ obtained from the binary tree of Figure 25 is transformed into a couple of words $(w_\bullet, w_\circ)$.

Figure 26 shows how to perform the transformation of $w_{\bullet\circ}$ to obtain the couple of words $(w_\bullet, w_\circ)$.

A.2 Sampling

Reciprocally, given two words $w_\bullet$ of length $(2j+1)$ on $\mathcal{A}_\bullet$ with i black-vertex-letters and $w_\circ$ of length $2i$ on $\mathcal{A}_\circ$ with j white-vertex-letters, we can first associate to this couple of words a word $\widetilde{w}_{\bullet\circ}$ of length $(2j+1)$ on $\mathcal{A}_{\bullet\circ}$ by doing the inverse operation of the operation represented on Figure 26. This word has the property that the sum of the weights of its letters is equal to -1. Then we search the unique word $w_{\bullet\circ}$ in the cyclic equivalence-class of $\widetilde{w}_{\bullet\circ}$ which has the "Dyck"-property, i.e. the sum of the weights of the letters of any of its strict prefixes is nonnegative. Finally, we associate to $w_{\bullet\circ}$ a binary tree of $\mathcal{B}'_{ij}$ by doing the inverse operation of Figure 25.

This method allows to sample objects of $\mathcal{B}'_{ij}$ and ensures that:

$$|\mathcal{B}'_{ij}| = \frac{1}{2j+1}\binom{2j+1}{i}\binom{2i}{j}$$